Structural and Functional Study of Hydrogenase Maturation Factor HypB from *Archaeoglobus Fulgidus*

LI, Ting

A Thesis Submitted in Partial Fulfillment
of the Requirements for the Degree of
Doctor of Philosophy
in
Biochemistry

January 2009

UMI Number: 3377959

INFORMATION TO USERS

The quality of this reproduction is dependent upon the quality of the copy submitted. Broken or indistinct print, colored or poor quality illustrations and photographs, print bleed-through, substandard margins, and improper alignment can adversely affect reproduction.
In the unlikely event that the author did not send a complete manuscript and there are missing pages, these will be noted. Also, if unauthorized copyright material had to be removed, a note will indicate the deletion.

UMI®

UMI Microform 3377959
Copyright 2009 by ProQuest LLC
All rights reserved. This microform edition is protected against unauthorized copying under Title 17, United States Code.

ProQuest LLC
789 East Eisenhower Parkway
P.O. Box 1346
Ann Arbor, MI 48106-1346

Thesis/ Assessment Committee

Professor K.B. Wong (Thesis Supervisor)

Professor C.C. Wan (Chairman)

Professor W.N. Au (Committee Member)

Professor G. Zhu (External Examiner)

Acknowledgements

This thesis could not be finished without the help and support of many people who are gratefully acknowledged here.

First and foremost I'm honored to express my deepest gratitude to my supervisor, Dr. Kam Bo Wong who led me into the wonderful world of protein structural crystallography. He offered me the insightful guidance, earnest help and constant encouragement. I have benefited from him a lot not only about the profound knowledge, but also the precise thinking. Without his illuminating instruction and consistent encouragement, I don't think I can accomplish this thesis by my own.

My special thanks should be given to all my diligent and brilliant labmates for their valuable suggestions and zealous assistances, Mr. Kwokho Chan, Mr. Kaming Lee, Miss Sonia Lam and Mr. Eric Chan and other members in MMW 507. I'm also extremely grateful to my friends, Ms. Geng Hua and Miss Linda Chong, for always being there to listen, offer support and make me smile when encountered difficulties in study or living.

Last my thanks would go to my beloved family for their unwavering support and unconditional love throughout these 4 years. Without their encouragement, I could hardly persist in pursuing my dream.

Abstract

The assembly of the [NiFe]-hydrogenases requires incorporation of Ni ions into the enzyme's metallocenter, which process requires the GTPase activity of HypB and HypA. Due to the essential role in assembly of the active site of hydrogenases, the two proteins were defined as hydrogenase maturation factors. To better understand the mechanism of GTP hydrolysis-dependent Ni delivery accomplished by HypB and HypA, our work focuses on the structure-function study of AfHypB from *Archaeoglobus fulgidus* and the functional interaction between AfHypA and AfHypB.

Up to now, we have solved the structure of apo-AfHypB by X-ray crystallography. Crystals of AfHypB were grown using the hanging-drop-vapor-diffusion method and diffracted to ~2.3 Å. It belonged to space group P2(1)2(1)2, with unit cell dimensions a=72.49, b=82.33, c=68.66 Å, $\alpha=\beta=\gamma=90°$. Two molecules of AfHypB were found in an asymmetric unit. Structural comparison between the apo-AfHypB and GTP-bound HypB from *M. jannachii* showed that the GTP binding broke the salt-bridge between K43 and D66, and induced conformational changes in the switch I loop and helix-3, which caused the HypB to form dimer and bind an extra Ni ion. The GTP-bound form of HypB was ready for Ni presenting. And GTP hydrolysis could induce the conformational changes of HypB in the switch I loop and helix-3, which dissociate the HypB dimer into the monomeric GDP-bound form.

The intrinsic GTPase activity of AfHypB is very low, suggesting that AfHypB requires a G-protein activating protein (GAP) to activate its GTPase activity. Although AfHypB can interact with AfHypA to form 1:1 heterodimer, our data suggests that AfHypA is not a GAP for AfHypB. In addition, the FRET results showed that AfHypA could serve as a GEF (G-protein exchange factor) to activate the AfHypB from GDP-bound form to GTP-bound form and facilitate the dissociation of AfHypB dimer in the presence of GMPPNP.

Furthermore, two Ni binding sites were determined in a monomeric HypB. One is the cluster including C92, H93 and C122, the other is composed of H97 and H101. Upon GTP-dependent dimerization, HypB can bind an extra Ni ion. Our results have shown that the C92/H93/C122 is involved in binding the extra Ni ion, and such binding requires both cysteine residues in the reduced form. Since the GTP-induced dimerization of HypB is coupled to bind an extra Ni, so HypB could act as a GTP-mediated switch that regulate one Ni release from the GTP-bound form to the GDP-bound form.

Based on what we have found, we proposed a model for Ni presenting by HypB involved in hydrogenase maturation. HypB binds two Ni ions in the apo- and GDP-bound form. Ni binding also induces dimerization of HypB. Upon GTP binding, HypB can bind an extra Ni ion at the dimeric interface. GTP hydrolysis will release the extra Ni ion, which may be subsequently inserted into hydrogenases during the maturation process.

In the future, we will attempt to crystallize AfHypB in complex with GDP, GTP analogue and AfHypA. Availability of good quality crystals will pave way for the structure determination of AfHypA and AfHypA/HypB complex. And the results obtained will provide a better understanding of the mechanism of functional interaction between HypA and HypB and how HypA and HypB play a role in Ni ion delivery for hydrogenase maturation.

摘要

镍铁氢化酶的组装需要将镍离子插入酶的活性中心。这个过程需要两个蛋白的参与，HypA 和 HypB。其中，HypB 是 GTP 磷酸酶。鉴于两个蛋白在氢化酶活性中心组装中的重要作用，我们将其称之为氢化酶成熟因子。为了更好地了解依赖于 GTP 水解的镍离子传递机制，我们将重点研究 HypB 结构与功能的相互关系以及 HypA 与 HypB 的功能相关性。

通过 X 光衍射学，我们已经解了 AfHypB 的晶体结构。我们用悬滴蒸汽扩散法获得结晶，可以衍射到大约 2.3 Å。此晶格属于 P2(1)2(1)2，晶胞大小为 a=72.49, b=82.33, c=68.66 Å，alpha，beta，gamma 都等于 90 度。每个不对称单位里面有两个 AfHypB 分子。我们将比较并讨论 apo-AfHypB 与 MjHypB/GTP-γ-S 在结构上的差异。

光衍射法可用于测定蛋白质的大小。由此方法确定 HypA 和 HypB 在自然状态下都是单体，但 HypB 在 GDP 结合状态和 GTP 结合状态下分别是单体和二聚体。此外，在自然状态和 GDP 结合状态下，HypB 与 HypA 可以按 1：1 的比例结合为异源二聚体。而在 GTP 结合状态下，倾向于形成异源四聚体。

为了研究 HypA 与 HypB 的相互作用对 HypB GTPase 活性的影响，我们分别测量了 HypB 与 HypA/B 复合体的 GTPase 的活性，并进行比较。结果发现，HypB 的基础活性很低，HypA 可以微弱激活 HypB。同时，我们还测量了 HypB 与 HypA/B 复合体对 GDP，GTP 等底物的结合能力。其结果表明，HypA 可以作为鸟嘌呤核苷酸交换因子（GEF）将 HypB 从 GDP 结合状态转换到 GTP 结合状态，并在一定程度上促使 GTP 结合的 HypB 二聚体解离。

此外，我们用平衡透析的方法测量 HypB 的镍离子结合能力。我们发现 HypB 在自然状态和 GDP 结合状态下，每个单体分子可以结合两个镍离子，

但在 GTP 结合状态下，每个二聚体分子可以结合五个镍离子。其中和传递相关的镍离子结合位点位于二聚体分子的接触面，由两个分子的 Cys92 和 Cys122 共四个半胱氨酸组成。这个位点在 GTP 水解后会消失，从而此位点结合的镍离子会释放出来，传递给氢化酶的活性中心。

在以后的研究中，我们会试图对 HypA，HypB 与不同的鸟嘌呤核苷酸底物，以及 HypA/B 复合体进行结晶，从而为研究它们的结构奠定基础，并能更好地了解 HypA 与 HypB 功能相关性，以及它们在氢化酶装配中的重要作用。

Table of Contents

List of Abbreviations

A. fulgidus	*Archaeoglobus fulgidus*
AfHypB	*A. fulgidus* HypB
B. japonicum	*Bradyrhizobium japonicum*
BLAST	Basic Local Alignment Search Tool
DNA	Deoxyribonucleic Acid
DTNB	5,5′-Dithiobis(2-nitrobenzoic acid)
E. coli	*Escherichia coli*
EDTA	Ethylenediaminetetraacetic Acid
FRET	Fluorescence Resonance Energy Transfer
GAP	GTPase Activating Protein
GEF	Guanine Nucleotide Exchange Factor
G protein	Guanine Nucleotide Binding Protein
H. pylori	*Helicobacter pylori*
HEPES	4-2-Hydroxyethyl-1-Piperazineethanesulfonic Acid
Hyp	Hydrogenase Pleiotropy
K_d	Dissociation Constant
LS	Light Scattering
MALS	Multiple-Angle Light Scattering
mant-nucleotides	2′-(or-3′)-O-(N-methylanthraniloyl) nucleotides
mGDP	mant-GDP
M. jannaschii	*Methanocaldococcus jannaschii*
MjHypB	*M. jannaschii* HypB
PCR	Polymerase Chain Reaction
PMSF	Phenylmethylsulfonyl Fluoride
RI	Refractive Index
SDS-PAGE	Sodium Dodecyl Sulfate-Polyacrylamide Gel Electrophoresis
SEC	Size-Exclusion Chromatography
TCEP-HCl	Tris(2-Carboxyethyl) phosphine Hydrochloride

Abbreviations of amino acids

A	Ala	Alanine
C	Cys	Cysteine
D	Asp	Aspartate
E	Glu	Glutamate
F	Phe	Phenylalanine
G	Gly	Glycine
H	His	Histidine
I	Ile	Isoleucine
K	Lys	Lysine
L	Leu	Leucine
M	Met	Methionine
N	Asn	Asparagines
P	Pro	Proline
Q	Gln	Glutamine
R	Arg	Arginine
S	Ser	Serine
T	The	Threonine
V	Val	Valine
W	Trp	Tryptophan
Y	Tyr	Tyrosine

List of Figures

List of Tables

Chapter 1

General Introduction

Hydrogenases catalyze the interconversion of molecular hydrogen into protons and electrons. Dependent on their metal content, hydrogenases are classified into two types: [NiFe]-hydrogenase and [Fe]-hydrogenase. [NiFe]-hydrogenase is the most widely distributed hydrogenases, which is found in organisms ranging from archaea to bacteria. Maturation of [NiFe]-hydrogenase requires the insertion of Fe, followed by Ni, to the active site center of the enzyme. These processes are assisted by maturation factors encoded by the hydrogenase pleiotropy operon hypABCDEF. Among them, Ni ions incorporation to the enzyme's active site is driven by GTP hydrolysis catalyzed by a hydrogenase maturation factor HypB and HypA, which are the study objects in this project.

1.1 Hydrogenase

Hydrogenases play vital roles in anaerobic metabolism (Frey 2002), which were firstly discovered in the 1930s. By utilizing hydrogen, the hydrogenase provides the bacterium a compact and high energy non-carbon substrate for respiratory- based energy generation (Olson and Maier 2002). Understanding the catalytic mechanism of hydrogenase might help scientists to design clean biological energy sources, such as hydrogen produced by algae.

1.1.1 Origination and definition

Hydrogenase is an enzyme widespread in prokaryotic and lower eukaryotic organisms (Vignais, Billoud et al. 2001).

Hydrogenases catalyze the reversible oxidation of molecular hydrogen and play a central role in microbial energy metabolism, which supply the molecular hydrogen as a source of energy or to use the protons as a receptor for excess reducing products ($H_2 <-> 2H^+ + 2e^-$) (Vignais, Billoud et al. 2001).

Now this reaction for the production or consumption of the molecular hydrogen is more important in biotechnological application.

1.1.2 Biotechnological applications

Previously, investigation of hydrogenase mainly focused on the traditional physiological and biochemical aspects to present the cellular functions of hydrogenases. Recently, a shifted emphasis was apparent in the widespread use of molecular biology and genetics.

Now hydrogenase is widely used in many biotechnological applications, including hydrogen production, wastewater treatment, the prevention of the microbial-induced corrosion and the generation and regeneration of NADP cofactors (Liese 2004).

The current interest is hydrogen acts as an alternative to fossil fuels, resulting in the exploration of the potential use of hydrogenase in biological production of H2 (Vignais and Colbeau 2004).

1.1.3 Classification of hydrogenases

Hydrogenases belong to the group of metalloenzyme diverse in structure and function. According to the metal content at their active sites, the hydrogenases are divided into three phylogenetically distinct classes: [NiFe], [FeFe] and metal-free (Vignais, Billoud et al. 2001). Hydrogenases contain an iron-sulfur cluster mostly with two metal atoms at the active site, either a Ni and an Fe for [NiFe]-hydrogenase or two Fe for [FeFe]-hydrogenase. However, the "metal-free" hydrogenase contains neither iron-sulfur cluster nor Ni atom. However, recent study showed that a member of "metal-free" hydrogenases, Hmd contains iron. Therefore, this type is more accurately to term as "FeS-free" hydrogenase.

Among these, the [NiFe]-hydrogenases are mostly widespread. So there is much significant progress in revealing the assembly process of the hydrogenase active site and identifying and characterizing the accessory proteins.

1.1.4 [NiFe]-hydogenase structure

The [NiFe]-hydrogenases are heterodimeric proteins composed of small and large subunits (Fig 1.1). The small subunit contains three iron-sulfur clusters while the large subunit contains a nickel-iron centre. The metal center of hydrogenases consists of an iron atom and a nickel atom hooked to four cysteine thiolate of the protein backbone of the large subunit, two of which serve as ligands bridging the two metals (Volbeda, Charon et al. 1995). In addition, the iron atom carries two cyano (CN) and one carbonyl (CO) ligand (Happe, Roseboom et al. 1997) (Volbeda A 2003).

The distinct character of the hydrogenase is the metallocenter. The majority of the hydrogenases contain iron-sulfur clusters and two metal ions at the active site. For the [NiFe]-hydrogenase, there is one Ni and one Fe, whereas for the [FeFe]-hydrogenase, two Fe ions existed (Vignais, Billoud et al. 2001).

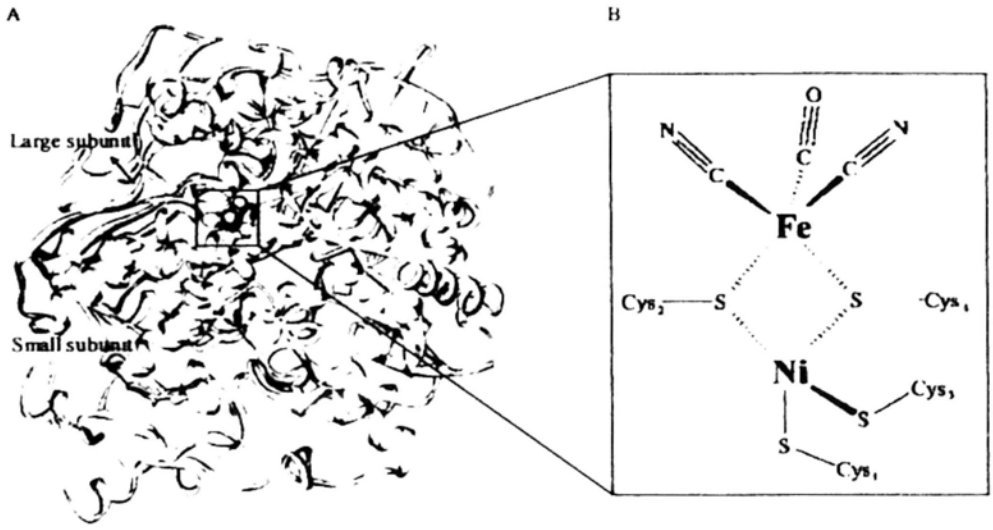

Figure 1.1 Structure of [NiFe]-hydrogenase from *D. gigas*. (A) The structure of [NiFe]-hydrogenase. The active site buried deeply is electrically linked to the surface via a chain of three [Fe-S] clusters. (B) The active site of [NiFe]-hydrogenase. The catalytic center of the [NiFe] enzyme composed of a Ni ion linked to four cysteines is located in the large subunit of the dimeric protein. Among the four cysteines, two of which also link to an iron ion that is bridged to one CO and two CN ligands as well.

1.2 Accessory proteins involved in biosynthesis of hydrogenase

Since the toxicity of the metal ions and the intricacy of the assembly of the metal center, a strict cellular control is required. So a series of proteins contributes to deliver the metal ions and assembly the metalloenzyme centers. These proteins direct the synthesis and incorporation of the metal ion to the metallocenter, and retain the fidelity of insertion the metal correctly into the active site of hydrogenase as well (Blokesch, Paschos et al. 2002).These proteins have been assigned to the hydrogenase pleiotropy (hyp) designation in many organisms.

1.2.1 Hyp operon

Biosynthesis of the [NiFe]-hydrogenase *in vivo* requires multiple accessory proteins that sequentially assemble the active site. These proteins have been identified by

isolating the mutant strains with deficient in the maturation of *E. coli* hydrogenase (Jacobi, Rossmann et al. 1992). The mutation map is addressed and sequenced, resulting in *hyp* (an abbreviation of hydrogenases pleiotropic genes) operon involved (Waugh and Boxer 1986; Lutz, Jacobi et al. 1991). The *hyp* operon is composed of five genes termed as hypABCDE with another separated gene hypF. Operon similiar to that of *E. coli* are also found in other organisms. The mutant strains of *hyp* operon lead to accumulation of the hydrogenase precursor, indicating of the role of these gene products in maturation of the hydrogenase (Binder, Maier et al. 1996).

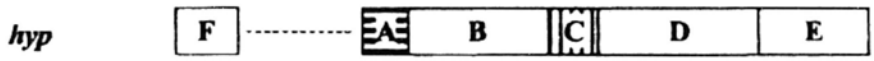

Figure 1.2 Organization of the hyp operon.

1.2.2 Roles of accessory proteins in maturation process

The assembly of metallocenter of [NiFe]- hydrogenase 3 in *E. coli* requires the participation of proteins encoded by the *hyp* genes hypABCDEF (Blokesch, Paschos et al. 2002).

Mutagenesis analysis indicated that the hypB, hypD, hypE and hypF were involved in the maturation of three kinds of hypdrogenase in *E. coli*, although hypA and hypC genes are only required for hydrogenase 3 (Jacobi, Rossmann et al. 1992). HypA and HypC are replaced by the homologous HybF and HybG respectively for the assembly of hydrogenases 1 and 2 (Casalot and Rousset 2001).

In *E. coli*, all of the hydrogenases belong to the class of [NiFe]-hydrogenase containing one Ni, one Fe and three organic ligands buried deeply in the active site (Mulrooney and Hausinger 2003). Such a complex metallocenter to synthesis requires multiple accessory proteins. These factors modulate a cascade of events, including gathering and transport of organic and inorganic ligands, construction of the metallocenter, GTP hydrolysis and protein folding and proteolysis (Kuchar and

Hausinger 2004). But many proteins have not been identified and characterized completely. Table 1.1 gives a summary of the complement of accessory proteins involved in hydrogenase maturation in *E. coli*, and also presents some structural characteristics of these proteins and their role in the maturation process.

Table 1.1 Properties of accessory proteins involved in the maturation of [NiFe]-hydrogenases from *E. coli* (Blokesch, Paschos et al. 2002).

Protein	Molecular mass (kDa)	Quaternary structure	Function
HypA/HybF	13/12.6	α_3	Ni insertion
HypB	31.4	α_2	GTPase, Ni insertion
HypC/HybG	9.6/8.7	α_2	Chaperone, Fe insertion
HypD	41.2	α	Fe–S protein, Fe insertion
HypE	33.6	α_2	CO/CN synthesis, ATPase
HypF	81.9	α	CO/CN synthesis, CP phosphatase, ATP pyrophosphorylase
Endopeptidases HyaD, HybD, HycI	21.4/17.6/16.9	α	C-terminal cleavage
CP synthetase (CarA/CarB)	41.3/117.6	$\alpha\beta$	Provision of CO/CN precursor

*A. Paschos, A. Bauer, A. Zimmermann, E. Zehelein and A. Böck, unpublished work.

1.2.2.1 HypC and HypD

HypC forms a complex with HypD to uptake the cyano group transferred from HypE (Blokesch, Albracht et al. 2004). HypD contains a [4Fe-4S] cluster. One of the Fe coordinates the cyanides and then is transferred to hydrogenase (Blokesch, Albracht et al. 2004). HypD is in an inactive form with the left [3Fe-4S] cluster.

HypC remains in a complex with the hydrogenase precursor until the Ni inserted. It has been suggested that pre-HycE (The large subunit of hydrogenase) incorporates Ni when formed a complex with a chaperone-like protein HypC prior to binding with the small subunit. HypC dissociated from the complex before the proteolytic processing of HycE, since only the HypC-free, Ni-containing form of preHycE can serve as the substrate of the endopeptidase (Drapal and Bock 1998; Magalon and Bock 2000; Magalon and Bock 2000).

1.2.2.2 HypE and HypF

[NiFe]-hydrogenases possess a Ni-Fe active site where the Fe has on CO and two CN as ligands. Synthesis of the CN ligands requires the two maturation factors: HypF and HypE, which modify carbamoyl-phosphate in two ATP-denpendent steps (Blokesch, Paschos et al. 2004). HypF is a carbamoyl-transferase that transfers the carbamoyladenylate to the carboxy-terminal cysteine of HypE and thus forms an enzyme-thiocarbamate. HypE dehydrates the S-carbamolyl group in the ATP-denpendent process to gain the enzyme thiocyanate (Reissmann, Hochleitner et al. 2003).

1.2.2.3 HypA/HybF and HypB

Both HypA and HypB participate in the Ni delivery to the active site of hydrogenase, which is supported by the fact that the stain deficient in hypA and hypB gene can be partially recovered by adding the Ni to the medium (Blokesch, Paschos et al. 2002).

E. coli HypB binds one Ni with a K_d in the picomolar range to the cysteines in the N-terminal CxxCGC motif, referred to as the high-affinity site (Leach, Sandal et al. 2005). In addition, both HypA and HypB bind a Ni with micromolar affinity. HypA contains a conserved His2, while HypB possesses several conserved residues in GTPase domain, termed as the the low-affinity site (Mehta, Olson et al. 2003; Atanassova and Zamble 2005). However, whether one or a combination of these binding sites serves as the Ni supplier for hydrogenase assembly has not been known yet.

A homologue HybF replace the HypA involved in hydrogenase 3 in the hydrogenase 1 or 2 (Kuchar and Hausinger 2004). In *E. coli*, the purified HybF is monomer containing stoichiometric amounts of Zn. But it can also bind Ni with a K_d of 1.87 μM. The mutant of H2Q abolish the Ni binding ability *in vivo* and *in vitro*, whereas can still bind stoichiomtric Zn. Substitutions of the four conserved cysteines in a Zn finger motif reduced the cellular amount of HybF without a loss of

in vivo hydrogenase activity, indicating that these residue only play a structural role for HybF (Blokesch, Rohrmoser et al. 2004).

1.2.3 Network of hydrogenase maturation

Although the details of hydrogenase metallocenter assembly are not yet clear, the sequence of events has been demonstrated according to the biochemical and genetic studies of several organisms.

The maturation process of hydrogenase is a complicated procedure, which requires many accessory proteins, which is encoded by hyp genes, HypA, HypB, HypC, HypD, HypE, HypF and an endopeptidase (Fig. 1.3). Only these proteins can guarantee the accuracy of the assembly and diminish the harm of the inorganic and organic elements (Kuchar and Hausinger 2004).

1.2.3.1 Synthesis of CN and CO

Synthesis of CN or CO ligand is performed by HypE and HypF (Reissmann, Hochleitner et al. 2003). HypF contains characteristic sequence of o-carbamoyl transferases and acyl-phosphatases, which are required for synthesis of the active center of hydrogenase and supplying the CO and CN ligands to Fe atom (Paschos, Glass et al. 2001). After uptaking the substrate of the carbamoyl phosphate (CP), HypF catalyzes a CP-dependent hydrolysis of ATP to AMP and pyrophosphate (PPi) and generates an adenylated CP derivative (Paschos, Bauer et al. 2002). After then, the carbamoyl group of CP is transported to the C-terminal cysteine of HypE in the presence of ATP. Carbamoylation of HypE is followed by the ATP-dependent dehydration of the carbamoyl adduct producing cyanated HypE. The cyano group is transferred to iron. The CO ligand may be derived from the hydrolysis of CN ligand and transfer of the carbamoyl group to iron, followed by deamination (Reissmann, Hochleitner et al. 2003).

1.2.3.2 Fe insertion

It is possible that the Fe insertion is accomplished by HypC and HypD (Blokesch,

Paschos et al. 2002). The protein-bound ligands are then transferred to Fe carried by a HypC/HypD complex. HypD in here contains an Fe-S cluster. The chaperone HypC is in a complex with pre-HycE and is thought to deliver Fe to pre-HycE (Magalon and Bock 2000). The pre-HycE/HypC complex is then available to incorporate Ni.

1.2.3.3 Ni insertion

The two metal ions are sequentially assembled to the large subunit of the hydrogenase. The iron was inserted followed by nickel incorporation (Winter G 2005).

After HypC binding to the large subunit HycE, the HycE is in an available conformation to uptake Ni. HypB is a G-protein with the capacity of binding and hydrolyzing the GTP. In the presence of HypA, HypB delivers the Ni to HycE coupled to the energy release from the GTP hydrolysis. After Ni inserted, the HypC is dissociated from the HycE/HypC complex. The C-terminal tail is cleaved by endopeptidase HycI. Thus the process of Ni insertion is completed (Hausinger 1993).

Mutations in hyp genes deficient in the capability of Ni-binding result in the accumulation of the large subunit without proteolysis, indicating that Ni is required for the proteolytic cleavage (Rossmann, Sauter et al. 1994). Mutations in the hycI gene yielded a hydrogenase precursor containing stoichiometric Ni. Thus indicated Ni insertion is prior to proteolytic cleavage of HycI (Rossmann, Sauter et al. 1994).

1.2.3.4 Proteolysis of the C-terminal tail of pre-HycE

HypC remains associated with the large subunit of hydrogenase HycE while HypA and HypB facilitate insertion of the Ni to the active site. After dissociation of the HypC, the C-terminal tail of pre-HycE is cleaved by endopeptidase HycI, which removes a 32 amino acid fragment from C-terminal of pre-HycE only after Ni inserted. So it is possible that Ni serves as part of the recognition motif for the

endopeptidase HycI, and the processing of the [NiFe]-hydrogenase is completed following cleavage of a C-terminal fragment. The proteolysis is highly specific for Ni over Zn, since Zn prevents the proteolysis and inhibits the formation of the hydrogenase precursor in complex with the protease (Magalon, Blokesch et al. 2001). This proteolysis induces a conformational change, leading to the closedown of the bridge between the Ni and Fe by the cysteines at the most C-termial (Magalon and Bock 2000). Accordingly, the mature HycE is available to assemble with HycG. The biosynthesis of hydrogenase is completed by the formation of a heterodimer associated by the large subunit HycE and small subunit HycG.

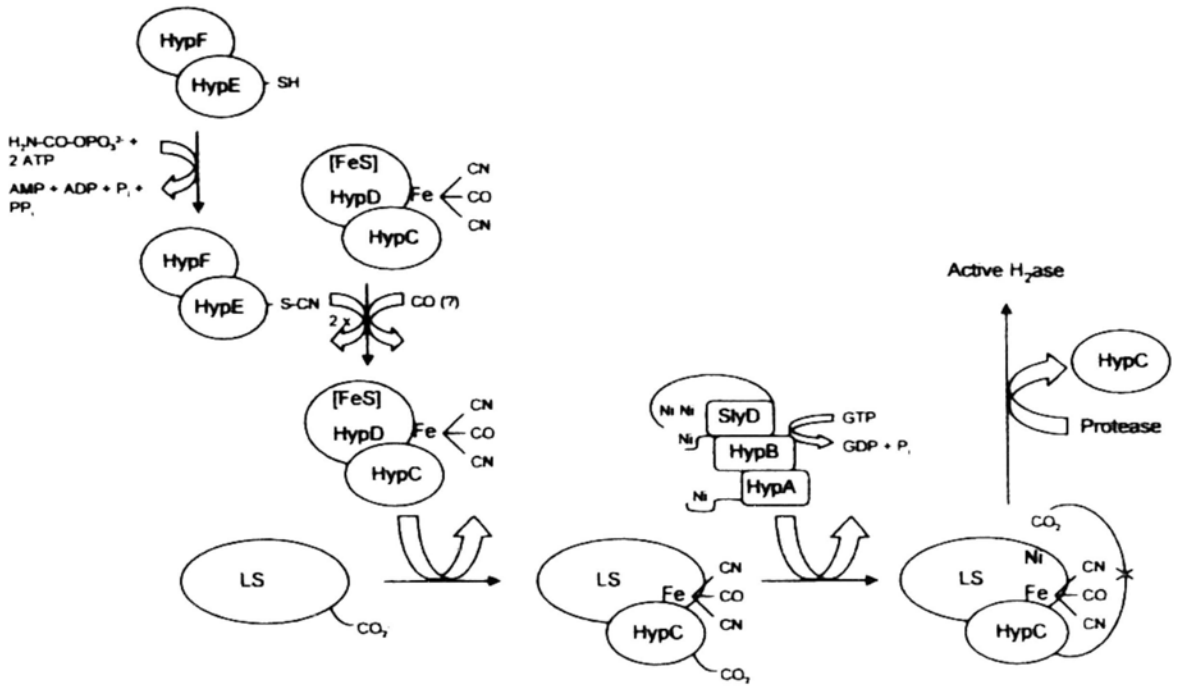

Figure 1.3 Postulated pathway of the maturation of hydrogenase 3 from *E. coli*. The biosynthesis of the E.coli hydrogenase 3 starts from the synthesis of the large subunit (HycE) as a precursor protein (pre-HycE) with an extension at C-terminal. HypCDEF participate in the biosynthesis and transport of the $Fe(CN)_2(CO)$ cluster to the hydrogenase precursor. The subsequent incorporation of Ni requires the GTPase HypB and HypA (Winter G 2005). HypC then remains associated with the HycE to facilitate GTP-dependent Ni insertion by HypB and HypA. The maturation process is ended by cleavage of the extension at C-terminal followed by binding the small subunit of HycG to produce active hydrogenase.

1.3 HypA and HypB for Ni enzyme maturation

A Ni-processing system is required for the fidelity of the Ni delivery. Some proteins constituted for the system are proposed to bind and assist to insert the Ni into the hydrogenase when it enters the cell. The characteristics and function of Ni-processing protein is described and model for Ni insertion into hydrogenase is presented.

1.3.1 Evidence for biosynthesis of the hydrogenase metallocenter

1.3.1.1 Requirement of HypA and HypB for the hydrogenase maturation

HypA and HypB are implicated in the step of production of the active hydrogenase from *E. coli* and *H. pylori* because deletions in either gene result in an Ni-deficient hydrogenase that is partially complemented by the addition of excess Ni, about 500 μL, to the growth medium (Waugh and Boxer 1986); (Jacobi, Rossmann et al. 1992); (Olson, Mehta et al. 2001). The HypB are known to play a role in Ni processing for the [NiFe]-hydrogenases of *E. coli, Azotobacter vinelandii, the Rhizobia spp.* and other organisms (Maier and Bock 1996). Mutations of conserved residues in the GTPase motifs of HypB that result in the loss of GTPase activity *in vitro* also abolish hydrogenase activity *in vivo* due to a lack of Ni loading, indicating that GTP hydrolysis is required for the transfer of a Ni into the large subunit of hydrogenase (Maier, Lottspeich et al. 1995).

1.3.1.2 Interaction of HypA and HypB

The finding of cooperation between HypA and HypB has been detected during the insertion of Ni to the hydrogenase (Hube, Blokesch et al. 2002). And an interaction between HypA and HypB in *H. pylori* has been determined by chemical crosslinking (Mehta, Olson et al. 2003).

1.3.1.3 Requirement of HypA and HypB for the urease maturation

In *H. pylori*, analysis of the mutants of the hypA and hypB genes has led to the surprising finding that both HypA and HypB are required not only for hydrogenase maturation, but also for urease maturation. The *H. pylori* genome contains the full accessory genes of both urease and hydrogenase. The mutant strain of hypA and hypB abolished the whole activity of hydrogenase and diminish the activity of urease in the meantime. Ni supplementation in media can restore the urease activity completely but partially recovery for hydrogenase (Olson, Mehta et al. 2001).

Further investigation suggests that both HypB and UreG (Homologue of HypB involved in the biosynthesis of the Ni-containing urease) contain a conserved

nucleotide-binding motif, GSGKT. Site-directed mutant of K59A in HypB eliminated the hydrogenase activity and possessed less then 1% of the wild type urease activity, which can be partially recovered for hydrogenase and fully recovered for urease by the Ni supplementation. Similar mutagenesis of K14A in UreG did not affect the hydrogenase activity, but abolished the urease activity, which can not be restored when Ni supplemented into the medium (Mehta, Benoit et al. 2003) .

1.3.2 Characteristics and functions of Ni-processing proteins

1.3.2.1 HypA

HypA has two distinct metal binding sites, one is a high-affinity Zn binding site and the other is a low-affinity Ni binding site. Ni binding is independent of Zn, indicating that two site have separated functions in the activity of HypA.

Studies on *H. pylori* HypA and *E. coli* HybF have shown that the N-terminal MHE motif is likely involved in the coordination of the Ni ion (Mehta, Olson et al. 2003; Blokesch, Rohrmoser et al. 2004). They are capable of binding Ni with affinity in a micro-molar range. In *H. pylori*, HypA possesses two Ni binding sites per dimer positive cooperatively with the K_1 and K_2 of 58 and 1.3 μM respectively. The conserved His2 is essential for Ni binding since the mutant in H2 of HypA abolish the hydrogenase activity and retain only 2% of the wild type urease activity (Mehta, Olson et al. 2003).

These proteins also contain a Zn binding site, which is located in a tetrathiolate coordination sphere with a structural role in the protein stabilization (Blokesch, Rohrmoser et al. 2004). This specific structural character is mostly found in protein domains that mediated the biomolecular interactions. So at this point, the HypA may act as an intermediated protein between the HypB and hydrogenase precursor and direct the Ni insertion into the hydrogenase (Atanassova and Zamble 2005). Accordingly, it is reasonable that the two homologues, HypA and HybF, are responsible for the respective hydrogenase (Blokesch, Rohrmoser et al. 2004). In

addition, HypA exist as dimer in the presence of Zn. Both HypA and HypB of *H. pylori* are homodimer, although form a heterodimer when interacted (Mehta, Olson et al. 2003).

A recent study of *H. pylori* HypA by X-ray absorption spectroscopy indicated a dynamic coordination environment around the Zn ion. Even if in the presence of Ni, the Zn is still bound in a tetrathiolate coordination sphere. However, in the absence of Ni, one of cysteine is substituted by an N or O donor. The Zn site of *H. pylori* undergoes a structural change in response to Ni binding, suggesting that it has a role in the specific binding of Ni (Kennedy, Herbst et al. 2007).

1.3.2.2 HypB

Recently, a crystal structure of the *M. jannaschii* HypB has been solved. This structure revealed a dimeric HypB in GTP-bound form is bridged by both an asymmetric dizinc cluster and the nucleotide binding site (Gasper, Scrima et al. 2006).

E. coli HypB contains two Ni binding sites. A high affinity binding site is located at N-terminal CxxCGC, which is a picomolar affinity binding site but not very conserved in the HypB homologues. It is suggested that this high affinity binding site might play a role only under selected growth conditions. The other binding site is in the GTPase domain with a micromolar affinity. This binding site is composed of several completely conserved residues and specific for Ni over Zn (Leach, Sandal et al. 2005).

In addition to the high-affinity binding motif of CxxCGC, some organisms possess a histidine-rich domain at N-terminal enables the HypB to store Ni, such as *Rhizobium leguminosarum*, *R. capsulatus*, *Azotobacter vinelandii* or *Bradyrhizobium japonicum* (Rey, Imperial et al. 1994; Fu, Olson et al. 1995; Olson, Fu et al. 1997; Olson and Maier 2000). Examination of the *B. japonicum* HypB demonstrated that a mutant lacking the His-rich region could still bind a single Ni

and maintain hydrogenase biosynthesis (Olson and Maier 2000), indicated that His-rich region appear to responsible for Ni storage and can be separated from the Ni insertion process (Mulrooney and Hausinger 2003).

AfHypB is one of the few homologues that does not contain either the N-terminal CxxCGC motif involved in high-affinity Ni binding or a polyhistidine stretch. Only the low affinity binding site in the GTPase domain is reserved in it.

1.3.3 Functions of GTPase

As for HypB, all proteins contain a conserved GTP-binding motif at the C-terminal to contribute the GTPase activity, which is shown to be requirement for Ni insertion (Maier, Lottspeich et al. 1995). It has been hypothesized that HypB in the GTP-bound state interacts with the Ni-free HycE and incorporate Ni to the active site (Maier and Bock 1996).

HypB from *Bradyrhizobium japonicum* contains a His-rich region with 24 histidine residues with a 39 residues stretch and a GTPase domain (Fu, Olson et al. 1995). *B. japonicum* HypB binds 9 Ni per monomer with a K_d of 2.3 μM and catalyzes the GTP hydrolysis (Fu, Olson et al. 1995; Olson, Fu et al. 1997). So the dual role in Ni storage and GTP-dependent Ni insertion are separated by functionally and structurally according to the respective domains of protein (Olson and Maier 2000).

1.3.4 GTP-hydrolysis dependent model for Ni insertion by HypA and HypB

From the results obtained so far, two models can be proposed for the function of HypA and HypB.

The first model is that HypA serves as a Ni chaperone, and HypB as a regulator that controls the donation of the Ni to the hydrogenase active site or release HypA after the Ni donated. The second is that HypB is the Ni-donating protein and HypA guides HypB to the apoprotein.

The former model is compatible with the fact that purified HypB protein from H. pylori does not bind Ni. Ni incorporation by HypA is initiated by the GTP-hydrolysis of HpHypB. The histidine located in the extreme N-terminus of HypA (His2) and the lysine in the GTP-binding motif of HypB (Lys59) play vital roles in Ni biding and GTP hydrolysis, respectively (Mehta, Olson et al. 2003).

The latter postulated model is supported by the fact that the conserved motif of the Ni binding site in the GTPase connects the Ni binding site and the γ-phosphate of the G-nucleotide (Gasper, Scrima et al. 2006), suggesting that the Ni binding is regulated by a GTP-mediated switch. In addition, the fact that HypA from E. coli functions only in the maturation pathway of hydrogenase 3 and there is a homolog of this protein, HybF, that has a role in the maturation of hydrogenases 1 and 2 instead (Hube, Blokesch et al. 2002). It is reasonable to assume that specific donation of Ni to the metal-free apoprotein requires recognition of the correct target by a protein-protein interaction. The fact that the sequences of the large subunits of isoenzyme1 and 2 are very similar to each other but very different from that of hydrogenase 3 (Vignais, Billoud et al. 2001) may have required the evolution of two separate Ni-delivering proteins.

In *E. coli*, HypA is a Zn-containing protein (Atanassova and Zamble 2005) but also binds stoichiometric amounts of Ni and HypB is a GTPase (Blokesch, Albracht et al. 2004). The high affinity site of HypB would serve as the Ni donor for hydrogenase. HypA would direct the Ni-bound HypB to the active site of the hydrogenase and facilitate the metal transfer. The model takes into account the weaker Ni-binding ability of HypA (compared to HypB), as important in facilitating the Ni-transfer step. The feasible role for the low-affinity metal binding site of HypB may detect the Ni status of the enzyme in order to sense when to activate the GTPase. Such an activation step upon sensing proper Ni loading would be of benefit, as HypB's have notoriously sluggish GTPase activities when tested in vitro (Leach, Sandal et al. 2005).

1.4 Organism of *A. fulgidus*

The HypB we studied comes from the *Archaeoglobus fulgidus*, which is a sulfhur-metabolizing organism. They are hyperthermophilic due to growing at extremely high temperature environment. Growth occurs between 60 and 95 °C, with optimum growth at 83 °C. Cells are irregular spheres with a glycoprotein envelope and monopolar flagella. The organism grows organoheterotrophically using a variety of carbon and energy sources, but can grow lithoautotrophically on hydrogen, thiosulphate and carbon dioxide (Klenk, Clayton et al. 1997).

1.5 Objective of this work

Hydrogenases and their maturation have attracted much research interests because of their potential biotechnological application in hydrogen production as an alternative fuel. In this project, the work mainly focuses on the study of a HypB protein, a maturation factor of hydrogenase, from *Archaeoglobus fulgidus*. Structure and biochemical properties of AfHypB will be studied. To understand how HypB performs its function as a G-protein, crystal structure of AfHypB will be solved by X-ray crystallography. The structure of AfHypB could provide a model for structural-function study of HypB. In the meantime, it will be compared to the previously solved model MjHypB to see if any information could be supplied by this new structure.

The affinity of AfHypB to its ligand GDP and GTP will be determined by FRET. Ni binding ability of AfHypB complex with GDP or GTP ligand will be studied by equilibrium dialysis. It will give us insight on how conformational change of HypB is related to the Ni binding ability upon GTP-hydrolysis. In addition, the interaction of AfHypB to AfHypA will be identified by pull-down assay. A purification system for HypA/B complex will be establish to study how does the HypA/B interaction affect the biological functions of HypB. Since the GTP hydrolysis by HypB is very essential for Ni incorporation into the hydrogenase precursor, so determination of the GTP hydrolysis effects on the conformational change of AfHypB and its functional interactions with AfHypA could provide insights into the role of HypA

and HypB played in Ni ion delivery. At last, a model for the functional HypB during Ni transport will be proposed.

Chapter 2

Materials and Methods

2.1 Reagents, plasmids and strains

Nucleotides were purchased as sodium salts from Sigma (St. Louis, MO).

Thrombin from bovine plasma from Sigma (St. Louis, MO).

For the malachite green assay (GTPase activity), the oxalate salt of malachite green, ammonium molybdate, sodium citrate tribasic dehydrate and Tween 20 were from Sigma (St. Louis, MO).

5,5′-Dithiobis(2-nitrobenzoic acid) (DTNB) suitable for determination of sulfhydryl groups from Sigma (St. Louis, MO).

2′-(or-3′)-O-(N-methylanthraniloyl) nucleotides (mant-nucleotides), dNTPs were from Invitrogen (Carlsbad, CA).

The restriction enzymes, Phusion™ High-Fidelity DNA Polymerase and T4 DNA ligase were purchased from New England Biolabs (Beverly, MA).

DNA purification kits were from Qiagen (Valencia, CA).

PfuTurbo® DNA polymerase from Stratagene (La Jolla, CA).

Molecular size markers were purchased from Bio-Rad Laboratories (Hercules, CA). Tris(2-Carboxyethyl) phosphine Hydrochloride (TCEP-HCL) from Thermo Fisher Scientific (Rockford, IL).

Micro-Equilibrium dialyzer and regenerated cellulose ultra-thin membrane from

Harvard Apparatus (Holliston, MA).

Expression vector pRSETA-HisMBP engineered previously in Prof. K.B. Wong's lab.

Escherichia coli (E. coli) competent cell strains DH5α, and BL21(DE3)pLysS were prepared for gene cloning and protein expression respectively.

Luria-Bertani (LB) medium or plates

Ampicillin (100 μg/ml)

Chloramphenicol (50 μg/ml)

Isopropyl-β-D-thiogalactopyranoside (IPTG) (0.2 mM)

2.2 General methods

2.2.1 Recombinant plasmid construction

The hypB gene was amplified by PCR with the genomic *A. fulgidus* genomic DNA as a template. All oligonucleotide primers were synthesized by Invitrogen™. The resulting 0.7 kb PCR product was digested with BamHI and EcoRI and agarose gel purified. The purified product was then ligated into the expression vector pRSETA-HisMBP (engineered by Prof. K.B. Wong's lab) previously cut with the same enzymes to generate the plasmid pHisMBP-hypB.

The hypA gene was amplified in the same manner. Both amplified hypA gene and plasmid pRSETA-HisMBP were digested with BamHI and EcoRI. The DNA fragment was inserted into expression vector pRSETA-HisMBP to generate pHisMBP-hypA.

Primers used for each gene were listed in the following Table:

Table 2.1 Primer used for each gene

Target gene	Primer	Primer sequence
AfHypA	Forward	5'TATGCAGGATCCATTATCAGAGATGTAGAA3'
	Reverse	5'TATGCAGAATTCTCAATTTTCTTTCAGTAA3'
AfHypB	Forward	5'TATGCAGGATCCAAAGTAAAGGAGGTCATA3'
	Reverse	5'TATGCAGAATTCCTATCGAAAGGCTTTGGC3'

2.2.2 Protein over-expression

The pHisMBP-hypB expression vector containing the hypB gene with an N-terminal HisMBP-tag was transformed to E. coli BL21(DE3)pLysS expression host (Novagen, Madison, Wis.). On the basis of the T7 expression system, large-scale expression of HisMBP-tagged HypB was achieved in 2 L of LB medium with 100 μg/mL ampicillin and 50 μg/mL chloramphenicol.

BL21(DE3)pLysS cells harboring a recombinant plasmid were grown at 37°C. When the OD600 reached 0.8, expression was induced by addition of IPTG to a final concentration of 0.2 mM and cells were grown for an additional 4 hours at 37°C and harvested by centrifugation (5,000 × g, 15 min, 4°C).

2.2.3 Protein purification

2.2.3.1 Cell lysis

Cells were harvested by centrifugation. The cellular pellet was resuspended in 20 mL of 20 mM Tris-HCl (pH 7.8) containing 500 mM NaCl, 10 mM imidazole (buffer A for Ni-affinity column). The protease of PMSF (Phenylmethylsulfonyl fluoride) was also added to a final concentration of 0.5 mM. The resuspended cell was lysed by sonication. Cell debris was removed by centrifugation at 12000 rpm × 30 min, and the supernatant was subjected to Ni-affinity column.

2.2.3.2 Ni-Affinity chromatography

The soluble fraction isolated by centrifugation was loaded onto a 5 mL HiTrap™ Ni-Chelating HP Column (GE Healthcare) pre-equilibrated with 20 mM Tris-HCl (pH 8.0) containing 0.5 M NaCl, 10 mM imidazole and 5 mM TCEP. The protein was eluted with a 100 mL linear imidazole gradient from 10 to 300 mM. Fractions were analyzed by SDS-PAGE, and proteins of interest were pooled.

2.2.3.3 Tag cleavage and separation

Following proteolysis with thrombin, the HisMBP-tag was removed by HiTrap Q anion-exchange column (GE Healthcare). HypB was eluted with a linear gradient from 0 to 0.5 M NaCl.

2.2.3.4 Gel filtration chromatography

The fractions containing HypB were combined, concentrated using 10 kDa Amicon_Ultra (Millipore) to a final volume of 5 mL, and clarified by filtration (0.22 μm) to remove the precipitated material. The solution was loaded onto a HiLoad 26/60 Superdex 75 column equilibrated with 20 mM Tris-HCl buffer (pH 7.8) containing 0.2 M NaCl and 5 mM $MgCl_2$ and 5mM TCEP. HypB was eluted at a flow rate of 3 mL/min. The eluted fractions containing the protein were analyzed by SDS–PAGE, pooled, and concentrated to 15 mg/mL. The protein was aliquoted and stored at -80 °C.

Expression and purification of the HypA was performed as for HypB.

2.2.4 Gel electrophoresis analysis

2.2.4.1 SDS-PAGE

Protein purity and the apparent molecular was estimated by SDS-PAGE, by using a BioRad Mini-Protean II apparatus (Bio-Rad, Hercules, CA). Proteins were separated on 12.5% (w/v) acrylamide-bisacrylamide separating gels, stained using Coomassie Brilliant Blue R-250.

2.2.4.2 Native-PAGE

In the native condition, the relative molecular mass of purified protein or complex as well as the proteins' purity were determined on 12.5% polyacrylamide gel electrophoresis (Native-PAGE) with a Mini-Protean II apparatus. Proteins were visualized with Coomassie brilliant blue R-250.

2.2.5 Protein concentration determination

Protein concentrations were measured using a spectrophotometer and a value for the extinction coefficient ($\varepsilon 280 = 10980\ M^{-1}\ cm^{-1}$ for HypB) calculated from the amino acid sequence using the ProtParam website (http://au.expasy.org/tools/protparam.html).

2.2.6 Light scattering

An estimate of the absolute molecular mass of protein under native conditions was determined using a combination of size-exclusion chromatography (SEC) and MALS (multiple-angle light scattering).

Protein (150 µL, 3~4 mg/mL) in 50 mM HEPES (pH 6.8) containing 200 mM NaCl was loaded onto a Superdex-75 HR10/30 column (GE Healthcare), pre-equilibrated with the same buffer, and eluted at room temperature at a flow rate of 0.5 mL/min. The column was connected downstream to a multiple-angle laser light scattering DAWN EOS photometer (Wyatt Technology). Values of 0.185 for the refractive index increment (dn/dc) and 1.330 for the solvent refractive index were used. Molecular weights were determined from a Zimm plot. Data were analyzed using Astra version 5.1.7 (Wyatt Technology), following the manufacturer's instructions.

2.2.7 Site-directed mutagenesis

A double mutant with a reduced Ni binding stoichiometry was designed based on the crystal structure of the MjHypB (Gasper, Scrima et al. 2006). Two pairs of residues, Cys92 and Cys122, His97 and H101, were mutated to alanines. The mutagenesis was performed with by QuickChange using the primers listed in Table 2.2. The mutant was expressed and purified in the same way as the wild-type

protein.

Table 2.2 Sequence of the primers used for mutagenesis of AfHypB

C92A	Forward	5'CACGGGAAAGGAGGCACACCTCGATGCGCA3'
	Reverse	5'TGCGCATCGAGGTGTGCCTCCTTTCCCGTG3'
C122A	Forward	5'CGGCAATTTAATCGCACCAGTGGACTTTGA3'
	Reverse	5'TCAAAGTCCACTGGTGCGATTAAATTGCCG3'
H97A	Forward	5'TCACCTCGATGCGGCAATGATTTACCACCG3'
	Reverse	5'CGGTGGTAAATCATTGCCGCATCGAGGTGA3'
H101A	Forward	5'GCGCACATGATTTACGCACGCCTGAAGAAG3'
	Reverse	5'CTTCTTCAGGCGTGCGTAAATCATGTGCGC3'

The codons corresponding to the mutations are underlined.

2.2.8 Sequence search and alignment

Sequences of HypB were searched using the program BLAST (Basic Local Alignment Search Tool) (Altschul, Gish et al. 1990; Altschul, Madden et al. 1997) available at http://www.ncbi.nlm.nih.gov/BLAST. Multiple sequence alignments were performed on the remaining sequences using the ClustalW program (Altschul, Madden et al. 1997) and alignment optimization was carried out using information deriving from secondary structure predictions provided by the program JPRED (Cuff, Clamp et al. 1998), available at http://www.compbio.dundee.ac.uk/~www-jpred.

2.2.9 Determination of the concentration of free cysteine

A solution of protein of 960 μL in 20 mM Tris-HCl (pH 8.0), 15 μM was incubated with 40 μL of 10 mM DTNB at room temperature for 15 min. The absorbance at 412 nm was measured and was stable after this incubation time. The concentration of free cysteine thiols in protein was calculated using a standardization curve, obtained with standard cysteine concentrations ranging from 0 to 200 μM, under

identical buffer conditions.

2.2.10 GTPase activity (Malachite green method)

GTP hydrolyzing activity was measured using a colorimetric method. The assay is to determine the free phosphate generated by measuring the absorbance of a molybdate/malachite green/phosphate reaction complex at 635 nm (Van Veldhoven and Mannaerts 1987). The sensitivity is approximately 50 pmol of free phosphate detected.

The reaction mixture, containing 20 mM Tris-HCl (pH 8.0), 0.15 M NaCl, 5 mM $MgCl_2$, 2 mM GTP, and 5 μM HypB, in the presence of 5 mM TCEP, was incubated at 37 °C. Aliquots (50 μL) were removed at different incubation times. The phosphate concentration was determined by the malachite green assay (Lanzetta, Alvarez et al. 1979).

Stock reagents:

0.045% malachite green hydrochloride (MG)

4.2% ammonium molybdate in 4 N HCl (AM)

1.5% aqueous Tween 20

34% sodium citrate·2H2O (w/v)

Pi standard: 10 mM KH2PO4 (dried overnight at 100°C); appropriate dilutions were made from this stock and used for standards

Procedure:

3:1 mixture of MG and AM solutions. Mixed at least 20 min and then passed through Whatman No. 5 filter paper (MG/AM). This mixture was freshly prepared daily. Whthin 1 hour before each assay, 100 ml of this mixture was combined with 3 ml of 1.5% Tween 20. To 50 μl of sample, 800ul of the MG/AM/Tween 20 solution is added and mixed. After 1 min, 100 μl of the citrate solution is added and mixed. This solution can be read at 635 nm in a spectrophotometer after 30 min reaction at room temperature for full color development.

2.2.11 Fluorescence spectroscopy

Binding of was investigated through fluorescence resonance energy transfer (FRET). Fluorescence was measured at 20 °C with a Perkin–Elmer LS 50B fluorimeter (Perkin–Elmer Analytical Instruments, Norwalk, CT). Binding of fluorescent mant-nucleotides to protein was monitored by changes in fluorescence of tryptophan, which was measured with an excitation wavelength of 295 nm and a maximum emission spectrum of 440 nm. The reaction mixture contained about 3 μM protein, 20 mM Tris-HCl (pH 7.5), 50 mM NaCl 5 mM $MgCl_2$ and 5 mM TCEP. As a negative control, fluorescence was measured at the same concentrations of mant-nucleotides in the absence of the protein. For the fluorescence titrations, the mant-nucleotide was added from a 1 mM stock solution to the sample containing a fixed concentration of protein or no protein. The dilution was negligible (less than 1%). In the presence of protein, the measured fluorescence intensity, Y, is a combination of the fluorescence of bound and free mant-nucleotides according to Eq. (1):

$$Y=FL*L+(FEL-FL)*EL, \quad (1)$$

where EL is the concentration of the protein·mant-nucleotide complex, L is the total concentration of the mant-nucleotide added, FL and FEL are the fluorescence intensities of one mole of the mant-nucleotide alone and of one mole of protein·mant-nucleotide complex, respectively. FL was measured in a titration experiment in which the mant-nucleotide was added to the buffer in the absence of protein. EL is the solution of a quadratic equation describing the single site binding of mant-nucleotide to protein [Eq. (2)]:

$$EL=((L+E+Kd)-sqrt((L+E+Kd)2-4*L*E))/2, \quad (2)$$

In the above equation, L is the total concentration of the mant-nucleotide, E is the total concentration of protein, and K_d is the dissociation constant. K_d and FEL were then obtained by fitting the fluorescence data from the titration experiments using

Eq. (3) constraining the fit to L, E, and FL.

$$Y=FL*L+(FEL-FL)*(((L+E+Kd)-sqrt((L+E+Kd)2-4*L*E))/2), \quad (3)$$

Finally, the K_d values for GDP and GTP were measured indirectly by competition with mant-GDP. Titration of mant-GDP binding to protein was done as described above in the presence of various concentrations of GDP or GTP. The apparent K_d values for mant-GDP were plotted as a function of the GDP or GTP concentrations to yield the Kd values.

The titration curve was plotted as an increase in fluorescence with respect to the protein-free experiment versus the nucleotide concentration by using Kaleidagraph (Synergy Software).

2.2.12 Equilibrium dialysis and Ni determination

The ability of the purified recombinant proteins to bind nickel was determined by graphite furnace atomic absorption spectrophotometry (Varian AA-100) following equilibrium dialysis. Briefly, 6 to 7 μM protein was dialyzed against 20 mM Tris-HCl buffer (pH 7.8) containing increasing concentrations of $NiCl_2$ for 48 h at 4°C. After dialysis, the nickel concentration of the protein solution (bound plus free Ni^{2+}) and the dialysis buffer (free Ni^{2+}) was measured. The concentration of bound nickel was estimated by subtracting the two values.

2.2.13 Crystallization and structure determination

2.2.13.1 Crystallization

Protein was stocked in 20 mM Tris-HCl buffer, pH 7.8, containing 200 mM NaCl, 5 mM $MgCl_2$, and 5 mM TCEP and then concentrated to 10-15 mg/mL. The initial screening of HypB were carried out using the commercial kit of Crystal Screen™ (Hampton research, Aliso Viejo, CA), a set of the 96 best crystallization conditions for more than 1,000 biological macromolecules.

Optimal crystallization was performed by the hanging-drop vapor diffusion method by mixing 1–2 μL of protein solution and an equal volume of precipitant solution. The precipitant solution for crystallization of HypB consisted of 8% (w/v) polyethylene glycol (PEG) 4000, 0.1 M sodium acetate buffer at pH 4.6.

2.2.13.2 Data Collection

X-ray diffraction data were collected in all cases from crystals flash-frozen in a stream of nitrogen gas at 100 K using an Oxford Instruments Cryojet using 20% (v/v) (±)-2-Methyl-2,4-pentanediol (MPD) as a cryo-protectant.

Data were collected from a single crystal, using an R-AXIS IV++ IP detector and Cu Kα X-rays generated by a Rigaku MicroMax-007 rotating anode generator.

Diffraction data were processed using the Mosflm and subsequently handled using CCP4 (1994) and CNS software (Brunger, Adams et al. 1998). HypB belong to the space group P21212 with unit cell parameters of $a=73.14$ Å, $b=82.15$ Å, $c=68.59$ Å, $\alpha=90°$, $\beta=90°$, $\gamma=90°$.

2.2.13.3 Structure modeling and Refinement

The initial phase was determined by the molecular replacement method using Molrep of CCP4 program suite. Model was built by CCP4 program suite with two molecules in the asymmetric unit.

The program Coot was used for subsequent map interpretation and manual model building. The model was refined with REFMAC5 (Murshudov et al., 1997) to an R factor of 0.24 for all data in the resolution range of 10 to 2.3 Å (Rfree = 0.28 for 5% data).

Crystallographic calculations were performed with the CCP4 program suite. No restraints on the noncrystallographic symmetry were imposed during refinement.

Chapter 3

Crystal Structure of AfHypB

3.1 Introduction

GTPases act as a major signaling mechanism operating as molecular switches via the hydrolysis of GTP. They are involved in many important functions, e.g., mRNA translation, cell cycling and signal transduction.

HypB protein is one of the small GTPases sharing a common structural fold, with the central β-sheet flanked by α-helices. Residues involved in nucleotide binding are located in several conserved motifs. Upon binding of different nucleotides, structural changes happen in the switch I and switch II regions respectively. Structural change in those regions may contribute to the functions of the protein.

To better understand the structure-function of HypB, we obtained the crystal structure of AfHypB in apo-form. Sequences and structures were compared for apo-AfHypB and GTP-bound MjHypB with the aim of understanding the conformational change upon GTP accommodation and hydrolysis.

3.2 Over-expression and purification of AfHypB

Expression and purification is the first step for the structure-function study of HypB. HisMBP-AfHypB fusion protein was expressed in *E. coli* BL21(DE3)pLysS strain. After purification with Ni-chelating chromatography, the fusion protein was digested with thrombin to remove the HisMBP-tag. HiTrap Q anion exchange chromatography was used to separate the tag and the protein. In the final step, gel filtration chromatography was used for further purification. The purified protein was analyzed by SDS-PAGE. The yield for purified AfHypB was 10-15 mg/L.

3.3 Crystallization and data collection

Initial crystallization condition was screened using commercial kits (*e.g.* Crystal

Screen kit from Hampton Research). Crystallization condition was then optimized by systematic grid searching with various buffer conditions like pH, precipitation and protein concentration.

Crystals of AfHypB for diffraction data collection were grown in 8% PEG 4000, 0.1M sodium acetate buffer at pH 4.6 using hanging-drop-vapor-diffusion method. Cryo-protection was achieved by soaking the crystals in mother liquor with 20% (v/v) MPD for 10 seconds. The crystal was then loop-mounted and transferred into the cryo-stream of nitrogen at 110 K. X-ray diffraction data were collected on an R-AXIS IV++ imaging-plate system using a rotating copper-anode X-ray source (Rigaku MicroMax-007 with VariMax optics) and processed by the MOSFLM of the CCP4 program suite. Four crystals were mounted and diffraction data, each with 90 images, were collected at 1° oscillations, with an exposure time of 10 min and a crystal-to-detector distance of 200 mm. Four sets of data were scaled and merged to a resolution of ~2.3 Å with SORTMTZ, SCALA, and TRUNCATE of CCP4 sutie. The crystal belongs to space group P2(1)2(1)2, with unit cell dimensions $a=72.49$, $b=82.33$, $c=68.66$ Å, $\alpha=90°$, $\beta=90°$, $\gamma=90°$.

In order to achieve the HypB crystal in complex with GTP or GDP, we attempt soaking native crystals in solutions containing GDP or GMPPNP, a non-hydrolysable analogue of GTP. But the crystal quality and diffraction was significantly impaired. Co-crystallization of apo-HypB with GDP and GMPPNP was also tried but no crystal was obtained. One possible explanation is the conformational changes accompanying the nucleotide binding. In addition, we also attempt to achieve the Ni-bound form of HypB, but the crystals crack when soaked in 5 mM $NiSO_4$.

3.4 Modeling and refinement

Diffraction data of HypB in apo-form have been collected and processed with the resolution to 2.3 Å. The phase problem was solved by molecular replacement using

the structure of GTP-bound HypB from *M. jannaschii* as template. Two molecules of AfHypB were found in the asymmetric units.

After molecular replacement, the electron density map and atomic model were built and refined interactively using the program COOT and the REFMAC5 program. The progress of refinement was monitored by R_{free}- and R-factors. In present study, the R_{free} decreased to 28%. Data collection and processing statistics are given in Table 3.1. The structure of AfHypB in apo-form is shown in figure 3.1.

3.5 Overall structure

There are two molecules of AfHypB in the asymmetric unit. The two molecules of AfHypB are superimposable with a r.m.s.d. of 0.393 Å between equivalent Cα atoms. AfHypB is composed of a seven-stranded parallel β-sheet flanked by 11 α-helices (Fig. 3.1BC). A central β-sheet flanked by α-helices is a common structural fold of the small GTPase. The strand order is 7-6-5-1-4-2-3. The folding pattern of HypB is the same as that of other members of the SIMIBI (after signal recognition particle, MinD and BioD) class.

3.6 GTP binding motif

Although G-nucleotide is not observed in our structure of apo-AfHypB, analysis of the AfHypB sequence reveals a set of motifs characteristic of small GTPases, including the P-loop (Walker A), switch I, switch II (Walker B) and NKxD motifs. These features not only contribute to nucleotide binding and hydrolysis, but also mediate the conformational changes related to signaling and regulation (Leipe, Wolf et al. 2002).

3.6.1 P-loop (Walker A motif)

Walker A sequence G_{37}xxxxGKT_{44} (where x represents any residue) constitutes the P-loop involved in the binding of phosphates of GTP (Fig. 3.1). The P-loop is located at the site between the N-terminal β1-strand and the following α-helix. The presence of P-loop motif, normally found to be associated with ATP or GTP binding

and hydrolysis (Walker, Saraste et al. 1982), supports the fact that AfHypB proteins is GTPase.

3.6.2 Switch I

G-proteins are molecular switches, which change conformation via GTP hydrolysis. Some regions are particularly sensitive to the presence of the γ-phosphate, particularly in the switch I and switch II. The so-called "switch" regions undergo conformational change upon GTP binding. The sequence for switch I is very variable among the GTPase superfamily. In AfHypB, the switch I comprises a loop connecting the β2 to α3 and the beginning of α3. It includes the conserved D_{66}VVSKADYER$_{75}$ sequence. Switch I appears to be very flexible with high B-factor (Fig 3.2 B and C) in both chains of AfHypB in the asymmetric unit. In particular, the electron density of residues 67-83 in chain B is invisible, probably due to its high flexibility (Fig 3.2 A).

3.6.3 Switch II (Walker B motif)

Switch II contains the characteristic sequence motif D/ExxG (Walker B motif) and coordinates the γ-phosphate moiety of GTP and a bound Mg^{2+}. In AfHypB, the switch II is located at the extended loop connecting the β4 to β5. The conserved ExxG is observed, which is part of the switch II sequence E_{115}NVGNLICPVDFDL$_{128}$. The G118 in the D/ExxG motif is an essential residue of switch II. It could bind the γ-phosphate and promotes a conformational rearrangement of the following loop upon GTP hydrolysis. Another conserved aspartate is involved in binding a water-bridged Mg^{2+} ion (Walker, Saraste et al. 1982). The Cys122 within this segment constitutes the Ni binding site of C92/H93/C122 (Fig. 3.1A), so this loop could connect switch II with Ni binding site. In this structure, the switch I region is disordered, although the switch II region is well positioned to transmit structural changes at the GTPase active site to the adjacent Ni-binding site (Fig. 3.2).

3.6.4 NKxD motif

The specificity of G proteins to guanine is determined by the conserved NKxD motif located at the end of β6 strand (Bourne, Sanders et al. 1991). The lysine side chain stacks with the base, the aspartic acid residue forms a bidentate hydrogen bond to the N1 and N2 atoms, and the asparagine residue binds to the O6 and N7 atoms.

AfHypB has an unusual architecture of the guanine-binding site compared to other HypB proteins. In AfHypB, the aspartate in the NKxD motif is replaced by Ala165 (Fig. 3.3A). We have found that in our structure of AfHypB, there is a nearby Asp194 that can take the role of the conserved Asp involved in NKxD motif by forming the hydrogen bond to the N1 atom of the base (Fig. 3.3B). It is reasonable to suggest that the guanine specificity of HypB is unaltered even if the recognition site is unusual.

To verify the above assumption, we carried out the competition assay with GDP and ADP. The fluorescence of mant-GDP was enhanced upon binding to HypB when measured by FRET between HypB and the bound mGDP. As shown in figure 3.3C, addition of excess unlabelled GDP resulted in the loss of the fluorescence enhancement, which demonstrates that it could displace the bound mGDP. On the contrary, no significant fluorescence change was detected when ADP was added. These observations suggest that HypB could bind the guanine nucleotides specifically, but not adenine nucleotides.

3.7 Structural differences between HypB in apo-form and in GTP-bound form

The structure of GTP-γ-S bound form of MjHypB was determined (Gasper, Scrima et al. 2006). Since the active site residues of AfHypB and MjHypB are almost identical in sequence, the structural differences between our structure of apo-AfHypB and GTP-γ-S bound MjHypB will reflect the conformational changes occurred upon GTP binding. The structure of apo-AfHypB is in general superimposable to that of GTP-γ-S bound form of MjHypB, with a Cα rmsd value

of 0.69 Å. This is not surprising given the high sequence identity of 50.4% between MjHypB and AfHypB. The largest structural changes on HypB upon GTP binding are observed in the switch I region. In apo-form of AfHypB, the γ-phosphate binding of GTP is occupied by Asp66 from switch I, which forms a salt-bridge with Lys43 from the P-loop. Upon binding of GTP-γ-S, the γ-phosphate group, displacing the Asp66, forms a salt-bridge with Lys43. As a result, the switch I loop is pushed away from its nucleotide-free position, bringing the helix-3 to move closer towards the bound GTP (Fig. 3.4C). In particular, the invariant residue Asp72 now swings to a position to interact with the Mg^{2+}. In apo-AfHypB, conformation of helix-3 is stabilized by salt-bridges between Arg75 and the side-chain of Arg75 of helix-3 docks between the carboxyl group of Glu48 and Glu52 of helix-2. The large movement of helix-3 upon GTP binding breaks these interactions, and brings the Arg75 moving ~6.5 Å towards the bound GTP to form a salt-bridge with the α-phosphate group and Glu48. Our analyses suggest that the conformational changes upon GTP binding is triggered by breaking of the salt-bridge between Lys43 and Asp66 that holds the switch I loop to the P-loop. The fact that Lys43 and Asp66 are conserved in all HypB sequences confirms our views that they play crucial role in conformational changes upon GTP binding (Fig. 3.4C). Noteworthy, the switch I loop and helix-3 is the flexible in apo-AfHypB (Fig. 3.2), and such flexibility may facilitate the large conformational change induced by GTP binding.

3.8 Potential Ni binding sites of AfHypB

Sequence alignment of HypB from various organisms shows that HypB generally has one conserved Ni binding sites, consisting of two cysteine residues and one histidine residue (Leach, Sandal et al. 2005; Bock, King et al. 2006). In AfHypB, these residues are C92/H93/C122 (Fig. 3.5). In our structure, the Cys92 and Cys122 form a disulfide bridge, presumably due to oxidation during the course of crystallization. Cys122 is in the switch II region (Fig. 3.4B). AfHypB lacks CxxCGC binding site found in *E. coli* HypB but has an extra potential binding site consisting of H97/H101 (Fig. 3.5). These two potential Ni binding sites are located in the AfHypB structure as shown in figure 3.5. We will report the characterization

of the Ni-binding properties of AfHypB in Chapter 5.

3.9 Summary

The crystal structure of apo-AfHypB has been solved. HypB monomer has a globular shape with a central β-sheet flanked by α-helices. The strand order is 7-6-5-1-4-2-3, as observed in the SIMIBI class of GTPases. The structure of AfHypB shows two polypeptide chains in an asymmetric unit. Structural comparison between apo-form of AfHypB and GTP-γ-S bound-form of MjHypB reveals the major conformation changes are mainly in the P-loop and switch I. In apo-form, the nucleotide binding pocket is partially buried by switch I, which residues have high B-factors and are more flexible than the rest of the molecule. When bound GTP, the switch I is pushed away from the pocket and the salt bridge is broken between switch I and P-loop, which are rearranged to accommodate the relatively large GTP-γ-S/Mg^{2+}. In addition, the switch II region comprising the Ni-binding cluster indicated of the functional correlation between the GTP hydrolysis and Ni incorporation by HypB.

Table 3.1 X-ray data collection and crystallographic refinement statistics

	AfHypB
Space group	P21212
Unit cell parameters	
Dimension (Å)	a=72.49, b=82.33, c=68.66
Angels (deg.)	$\alpha=\beta=\gamma=90$
Resolution (Å)[a]	42.76-2.42 (7.27-2.30)
No. of observed reflections	235073
No. of unique reflections	18861
$I/\sigma(I)$ [a]	20.0 (5.4)
Completeness (%)[a]	100.0 (100.0)
Redundancy [a]	12.5 (7.9)
R_{merge} (%)[a]	10.7 (25.0)
R_{cryst} (%)	23.2
R_{free}, 5% data (%)	28.16
Molecules in asymmetric unit	2
Protein atoms	6131
Water molecules	56
Cl^- atoms	1
PEG molecules	1
Rmsd values	
Bond length (Å)	0.026
Bond angle (deg.)	2.075
Mean *B*-values ($Å^2$)	33.385
Ramachandran plot analysis	
Most favored region (%)	96.34
Additionally allowed region (%)	3.66
Other (%)	0
Missing residues	A: 1-10, 214-221 B: 1-8, 67-82, 211-221

[a] Numbers in parentheses indicate values for the highest-resolution shell.

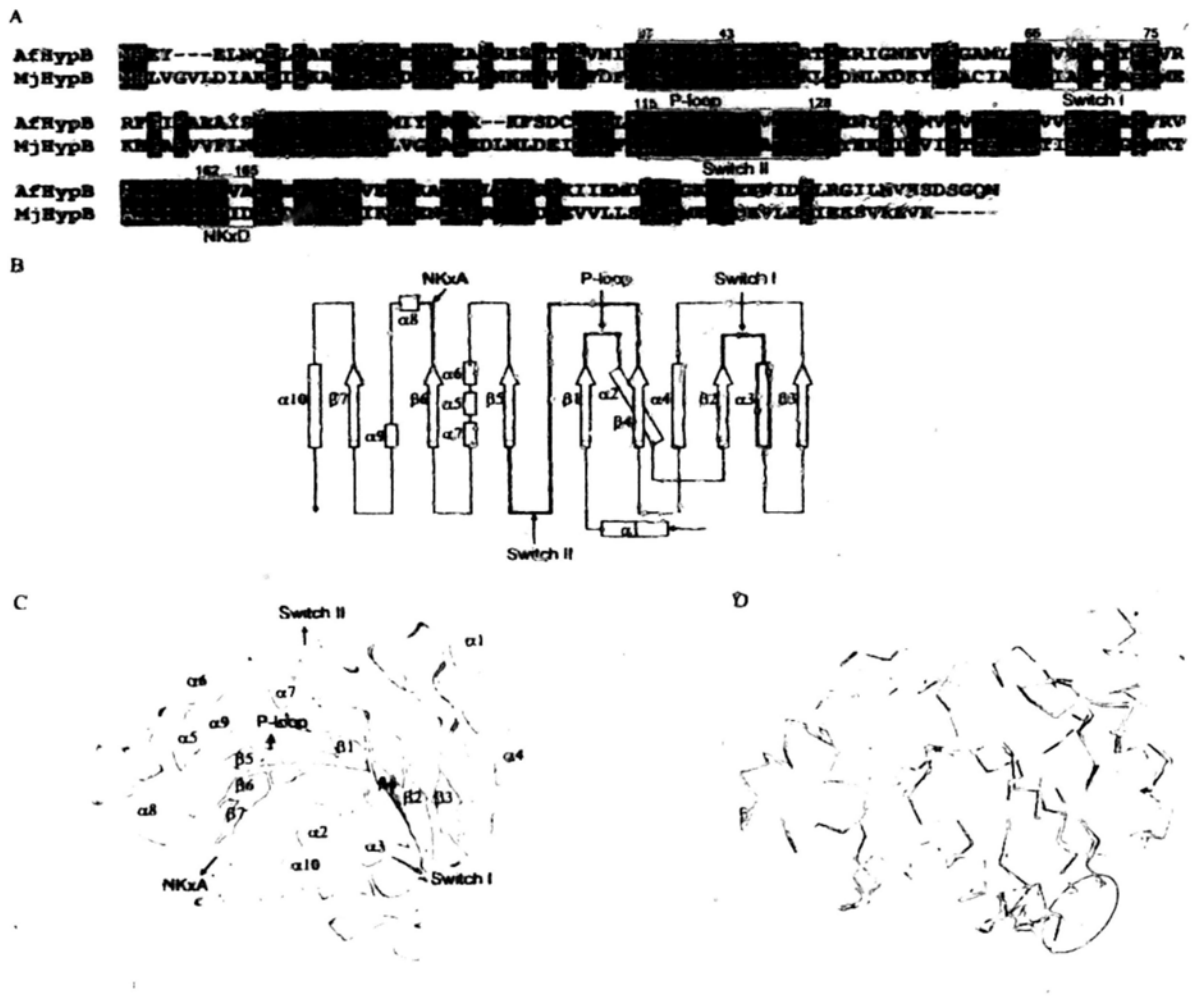

Figure 3.1 Structure of AfHypB. (A) Multiple sequence alignment of representative HypB sequences from *A. fulgidus* and *M. jannaschii*. The alignment shows four conserved GTP-binding motifs, the P-loop, switch I, switch II and NKxD. (B) Topology diagram of AfHypB. Helices are shown as rectangles. Strands are shown as arrows with the arrowhead on the C-terminus and numbered 1 through 7. Strands 1, 4, and 6 including the conserved sequence motifs GxxxGKT (P-loop), ExxG (part of switch II region) and NKxA (the GTP-specificity motif) are emphasized in bold. (C) Ribbon representation of AfHypB. The α-helices and β-strands are shown in yellow and green respectively. A central 7-stranded parallel β-sheet flanked by α-helices is a common structural fold of the small GTPase. (D) The superimposition of chain A and chain B of AfHypB. The loop following switch I of chain B is invisible in the electron density as indicated in red cycle.

Figure 3.2 Flexibility of AfHypB structure. (A) Superimposition of the structures of apo-AfHypB and the MjHypB/GTP-γ-S/Mg^{2+} complex (PDB accession, 2HF9). The ribbon tracing of AfHypB is presented in dark gray, while that of MjHypB/GTP-γ-S/Mg^{2+} is in light gray. The GTP and Mg^{2+} ion bound in MjHypB are displayed in ball-and-stick format with orange and magenta respectively. By comparing the two structures, the major conformation difference between the two states of HypB is the switch I region, which undergoes the significant conformational change upon GTP binding. The switch I regions in AfHypB and MjHypB are shown in green and yellow respectively. (B) The flexibility of chain A of AfHypB. The thicker line reflects the larger B-factor, indicating of high fluctuation of individual atoms and large conformational changes. The switch regions that communicated GTP hydrolysis, particularly in switch I, are more fluctuated. (C) The flexibility of chain B of AfHypB. The switch I of chain B is too flexible to define.

A

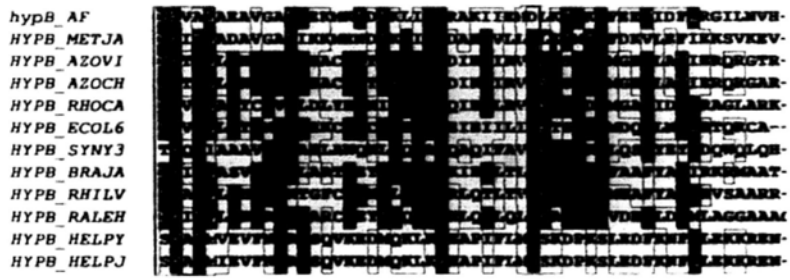

B

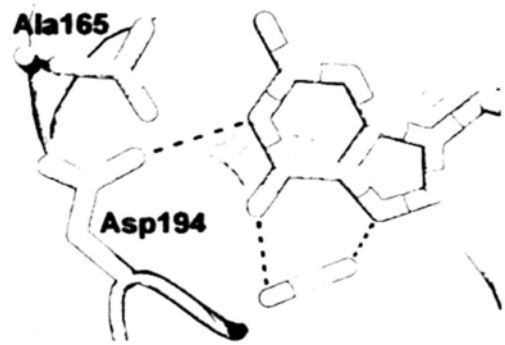

C

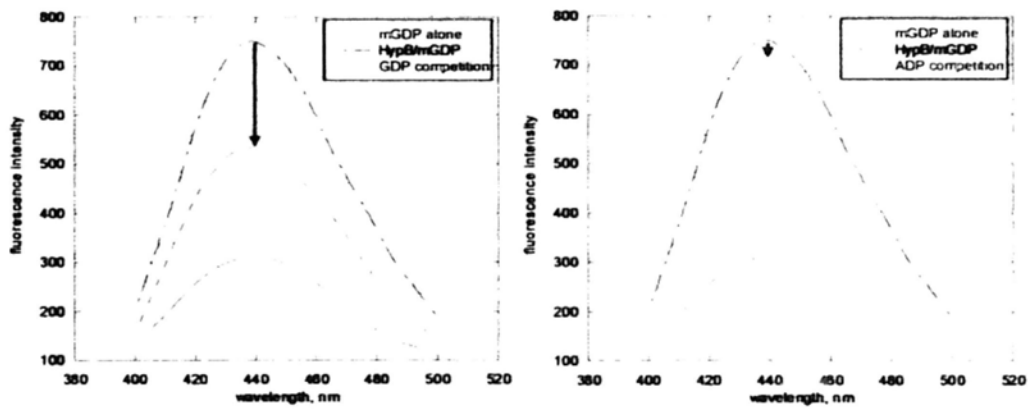

Figure 3.3

Figure 3.3 Specificity for guanine nucleotide binding to HypB. (A) Multiple sequence alignment of the NKxD motifs among the HypB proteins. AfHypB with the unusual NKxA motif is an exception to other HypB proteins. UniProtKB/Swiss-Prot entry names are indicated on the left. HYPB_AF, *Archaeoglobus fulgidus DSM 4304*; HYPB_METJA, *Methanococcus jannaschii*; HYPB_AZOVI, *Azotobacter vinelandii*; HYPB_AZOCH, *Azotobacter chroococcum*; HYPB_RHOCA, *Rhodobacter capsulatus*; HYPB_ECOL6, *Escherichia coli O6*; HYPB_SYNY3, *Synechocystis sp. strain PCC6803*; HYPB_RHILV, *Rhizobium leguminosarum biovar viciae*; HYPB_RALEH, *Ralstonia eutropha H16*; HYPB_HELPY, *Helicobacter pylori*; HYPB_HELPJ, *Helicobacter pylori J99*. (B) The GTP-recognition motif of HypB. In MjHypB, the conserved NKxD motif is involved in hydrogen bonds between Asp170 and the guanine N1 and N2 atoms as well as the Asn167 and O6, N7 atoms. The GTP-recognition motif in AfHypB is NKxA with invariant Ala165 instead of aspartate. However, Asp194 from another loop could compensate the deficiency of the conserved Asp involved in NKxD motif by forming the hydrogen bond to the N1 atom of the guanine base. Thus the guanine specificity for HypB is unaltered. (C) Specificity for nucleotide binding to HypB. The fluorescence intensity of mGDP with HypB is monitored at λ_{em} = 440 nm with excitation at λ_{ex} = 295 nm. The fluorescence emission spectra of mGDP before and after addition of HypB are indicated as red and black line respectively. Left panel: fluorescence emission spectra of mGDP with HypB before (black) and after addition of GDP (blue). The significant decrease of fluorescence indicated that the addition of an excess of GDP could displace mGDP bound to HypB; Right panel: fluorescence emission spectra of mGDP with HypB before (black) and after addition of ADP (green). The negligible decrease of the fluorescence indicated that the addition of an excess of ADP could not displace mGDP bound to HypB.

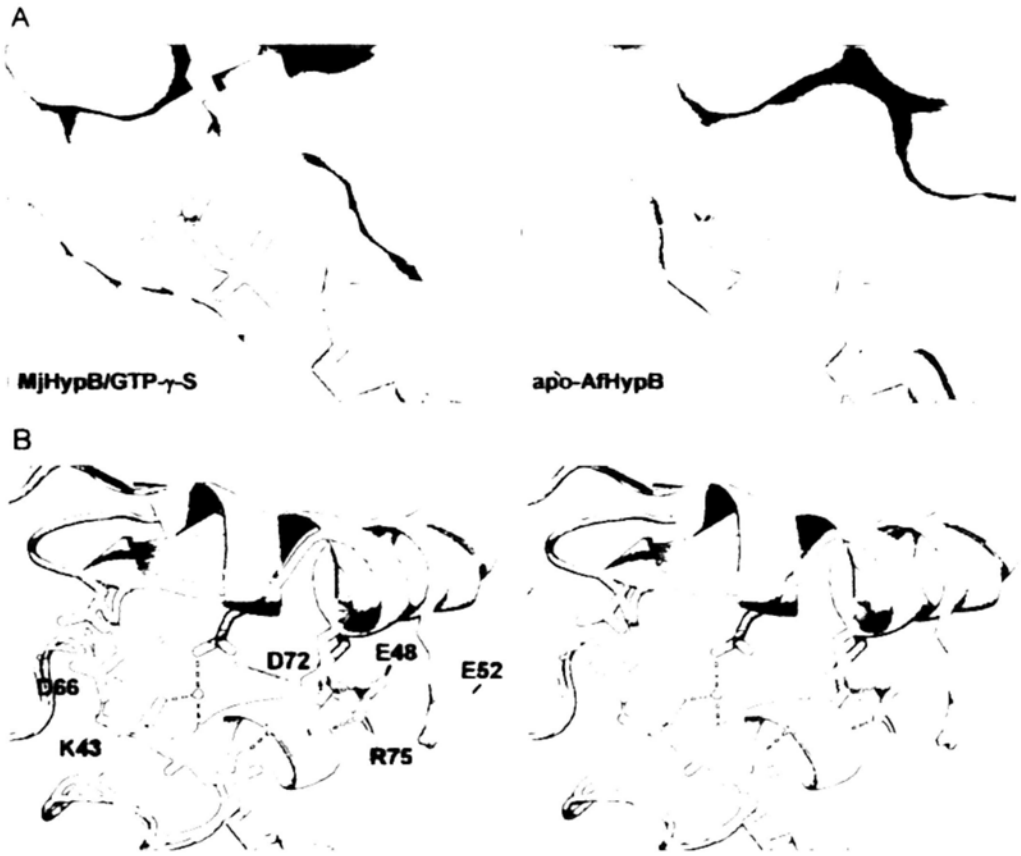

Figure 3.4 Structural comparison between the apo-form of AfHypB and GTP-γ-S bound form of MjHypB reveals major structural changes in the switch I loop region. (A) Surface representation of MjHypB/GTP-γ-S/Mg^{2+} and apo-AfHypB shows that the γ-phosphate binding pocket in apo-AfHypB is blocked by D66 (green), which forms a salt-bridge with K43. (B) Stereo diagram showing the conformational changes in the switch I loop and helix-3 upon GTP-γ-S binding. The residues in the P-loop and the switch I region of Apo-AfHypB are colored in cyan and green respectively, while GTP-γ-S-MjHypB is in dark-grey. Upon GTP binding, the γ-phosphate breaks the salt-bridge between D66 and K43, and pushes the switch I loop away from P-loop, bringing D72 and R75 of helix-3 to form multiple hydrogen bonds with the phosphate groups of GTP-γ-S. The movement of D66, D72, and R75 are indicated by green arrows.

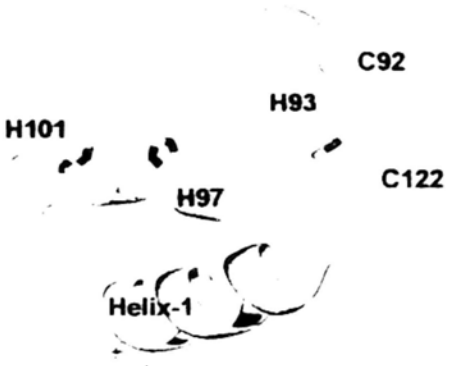

Figure 3.5 Ni binding sites of AfHypB. Two potential Ni binding sites exist in HypB monomer. One is composed of Cys92, His93 and Cys122, and the other is composed of His97 and His101.

Chapter 4

Interaction between AfHypB and AfHypA

4.1 Introduction

In vivo genetics studies in *E. coli* and *H. pylori* showed that inactivation of two genes resulted in reduction of hydrogenase activity, which can be restored by addition of high concentration of Ni (Waugh & Boxer 1986; Maier et al. 1993; Olson et al. 2001; Hube et al. 2002). The two inactivated genes are hypB and hypA (or its homologue hybF), so they are required for Ni insertion into hydrogenase. Moreover, it has been demonstrated that HypB could interact with HypA by in-vitro cross-linking experiments. The size of the cross-linked product suggests the two proteins form a 1:1 heterodimer (Mehta et al. 2003; Atanassova & Zamble 2005). Therefore, biosynthesis of active [NiFe]-hydrogenases requires a nickel insertion step assisted by hydrogenase maturation factors HypA and HypB.

The role of HypA/HypB interaction is currently not known. It may be required for directing the Ni insertion complex to the hydrogenase via protein-protein interactions, or the HypA/HypB complex may serve as a regulatory switch that change conformation upon GTP hydrolysis (Atanassova & Zamble 2005). So to clarify the functional interaction between HypB and HypA, we should confirm the interaction between the AfHypA and AfHypB at first.

4.2 HypB interacts with HypA

We cloned and expressed the recombinant hypA and hypB genes of *A. fulgidus* to gain further insight into the functional interaction between HypA and HypB and the effect of HypA on biological function of HypB.

4.2.1 Interaction of HypB with HypA determined by pull-down assay

The pull-down assay is an *in vitro* method used to study interaction between two or more proteins. The minimal requirement is the availability of a purified and tagged

protein, which can bind to the affinity column specific for the tag, therefore generating a "secondary affinity support" for capturing other protein-binding partners.

In this study, the interaction of HypA and HypB is investigated by MBP (maltose-binding protein)-tag pull-down assay. HypA was expressed as a fusion protein with the MBP-tag. It was immobilized on amylose agarose matrix that serves as a solid phase. After then, the purified HypB was loaded onto the column. Unbound material was washed off from the column, and subsequently the binding complex was eluted with maltose. The eluted proteins analyzed by SDS-PAGE with Coomassie blue staining consist of HisMBP-HypA and HypB (Fig. 4.1).

4.2.2 Formation of HypA/B complex *in vitro*

In addition to the pull down assay, we also perform another assay to confirm the interaction between HypA and HypB. Equal molar concentration of purified HypA and HypB were mixed at room temperature. After 15 min incubation, the mixture was subjected to native PAGE analysis. A slower mobility band was observed, indicating of HypA/B complex formation. The band corresponding to the complex were sliced from the native gel and re-loaded to SDS-PAGE. The retarded band identified by SDS-PAGE contained both HypA and HypB. The presence of two dissolved bands confirmed the formation of HypA/B complex (Fig. 4.2).

4.2.3 Preparation of HpyA/B complex

Firstly, HypA and HypB proteins were over-expressed as soluble proteins and purified to homogeneity respectively. The yield for both proteins was 10 to 15 mg/L. On SDS-PAGE gel, HypA and HypB migrated at approximately 12 and 25 kDa respectively.

After then, 2-fold excess HypA was incubated with HypB for 1 hour at 4°C in HEPES buffer. The incubated sample was concentrated and injected into a Superdex 75 column to remove the excess HypA from the HypA/B complex. The purified

protein complex was analyzed by SDS-PAGE and native-PAGE. Aliquots were stored at -70 °C to preserve the stability of the complex.

4.2.4 Stoichiometry of HypA/HypB complex determined by LS

Although the HypA/B complex formation was confirmed, the architecture of the complex has not been characterized. Therefore, the stoichiometry of HypA/B complex will be investigated by light scattering. A combination of size-exclusion chromatography (SEC) and multiple-angle light scattering (MALS) (Wen, Arakawa et al. 1996) is generally used to determine the absolute molecular mass. So it is very useful to determine the stoichiometry of the native state of a protein or complexes between different proteins.

In this study, purified proteins and complexes were subjected to SEC/LS analysis for the determination of their stochiometries. The protein samples were first fractionated by Superdex™ 75 column (GE Healthcare) and directed to the downstream detectors for recording the signals. The light scattering (LS) and refractive index (RI) signals were collected by two downstream detectors: miniDAWN and Optilab® DSP. The experiment was conducted under a flow rate at 0.5 mL/min at room temperature. Molecular weight of protein sample was obtained by calculating the acquired LS and RI data using ASTRA. Throughout the calculations, a dn/dc value of 0.185ml/g and fit degree of 0 were used.

4.2.4.1 Both HypA and HypB exist as monomer in solution

Purified protein was subjected to SEC/LS analysis. The sample with the concentration of 3 to 5 mg/mL was injected into Superdex™ 75 column pre-equilibrated with 50 mM HEPES, 0.2 M NaCl, 5 mM $MgCl_2$, 5 mM TCEP, pH 6.5. The SEC/LS analysis showed that the absolute molecular weight of HypA and HypB were 12 and 25 kDa respectively, which match to each theoretic molecular weight. Thus both HypA and HypB exist as monomer in solution (Fig. 4.3).

4.2.4.2 Stoichiometry of HypA/B complex is 1:1

Injection of the mixture of purified HypA and HypB resulted in a new peak that eluted before either of the isolated proteins, and analysis of this peak by LS revealed the molecular weight of the HypA/B complex is 37 kDa, which is just equal to the sum of that of each proteins. Therefore HypB formed a hetero-dimer with HypA within 1:1 molar ratio (Fig. 4.3).

4.3 GTP-dependent dimerization of HypB

It has been reported that GTP binding can induce dimerization of HypB (Gasper, Scrima et al. 2006). To investigate the GTP-dependent dimerization of AfHypB, we used SEC/LS to investigate the native molecular weight of HypB samples with and without addition of guanine nucleotides. As shown in figure 4.4, both apo-form and GDP-bound form of AfHypB were eluted as a monomer with a molecular weight of ~24 kDa, which matches to its theoretical molecular weight of 25 kDa. On the other hand, in the presence of GMPPNP, the AfHypB was eluted as a homodimer with a molecular weight of 47 kDa.

According to the results, AfHypB exists as a monomer in solution but dimerizes in the presence of GMPPNP. Our results are consistent with the dimerization of MjHypB upon GTP bidning. In the crystal structure of GTP-bound form of MjHypB, the bound GTP-γ-S molecules are tightly sandwiched in the dimer interface, which directly mediate the formation of homodimer (Gasper, Scrima et al. 2006). Our results support the conclusion that the GTP-dependent dimerization is a common feature of HypB proteins.

4.4 Dimerization of HypA/B complex upon GMPPNP binding

4.4.1 GTP binding induce dimerization of HypA/B complex

To see if interaction with HypA affects GTP-dependent dimeriztion of HypB, the binding of HypA and HypB in the presence of GDP or GMPPNP will be investigated by SEC/LS method.

Apo-form of HypB was mixed with excess amount of HypA. The mixture was pre-

incubated with and without 200 μM of GDP, and then injected into the Superdex™ 75 column equilibrated with the buffer containing equal molar of GDP. The SEC/LS result showed that the GDP-bound HypA/B complex formed a hetero-dimer with a molecular weight of 34 kDa (Fig. 4.5A). However, when the same sample pre-incubated with 200 μM GMPPNP, and injected into the Superdex™ 75 column equilibrated with the buffer containing GMPPNP, HypA/B complex was eluted earlier with a molecular weight of 49 kDa. Similar observations were obtained with a purified sample of apo-form and GDP-bound form of HypA/B complex (Figure 4.5 B, C).

4.4.2 HypA interaction weakens the dimerization of HypB

The measured molecular weight of 49 kDa lies between the expected molecular weight of a HypA/B complex (37 kDa) and that of a dimer of HypA/B complex (74 kDa). SDS-PAGE analyses confirm that elution peaks contain both HypA and HypB. To rule out the possibility of A/A/B and A/B/B complex, we have added excess GDP to the purified sample of GMPPNP-bound form of HypA/B complex. SEC/LS analysis showed that the GMPPNP-bound form of HypA/B was converted to 1:1 heterodimer of HypA/B without any excess HypA or HypB observed (Fig. 4.5D), suggesting that the molar ratio of HypA:HypB in the GMPPNP-bound form of HypA/B complex was 2:2. Our results also suggest that the conversion between the GDP-bound and GMPPNP-bound forms of HypA/B complex is reversible.

Taken together, we hypothesize that HypA/B complex will dimerize to form A/B/B/A complex upon GMPPNP binding. However, conversion between A/B and A/B/B/A complex is fast, and both HypA/B and dimer of HypA/B complexes exist in the equilibrium so that the observed molecular weight of 49 kDa represents a population average:

$$\underset{(37\ \text{kDa})}{\text{HypA/B} + \text{GMPPNP}} \leftrightarrow \underset{(74\ \text{kDa})}{\text{HypA/B/B/A\_GMPPNP}}$$

Our hypothesis predicts that increasing concentration of GMPPNP should favor the

dimerization of HypA/B complex, and increase the apparent molecular weight measured. To test this hypothesis, we have measured the apparent molecular weight of HypA/B complex with different the concentration of GMPPNP (100, 200, 1000 μM). Agreeing with our hypothesis, our results showed that in response to increasing concentration of GMPPNP from 100 μM to 1 mM, the measured molecular weight of HypA/B complex increased from 45 kDa to 56 kDa (Fig. 4.6), while the measured molecular weight of HypA/B complex is independent of GDP concentration (Table 4.1).

Based on the differences between the measured and the expected molecular weight, we can estimate the dissociation constant of HypB dimerization upon GMPPNP binding (Table 4.1). At 100 μM GMPPNP, the measured molecular weight of HypB is 47 kDa, suggesting that there should be >90% of HypB is present as a dimeric form, which translate to an estimated value K_d of <2 uM. On the other hand, in the presence of HypA, the estimated K_d value was increased to ~250-300 μM. Our results support a model that HypA induces the dissociation of GTP-induced HypB dimer.

4.5 Summary

Our results showed that HypB existed as a monomer in apo-form and GDP-bound form, but formed a homodimer in GTP-bound form. Pull-down assay and SEC/LS analysis has demonstrated that AfHypA and AfHypB interact with each other to form a 1:1 heterodimer in their apo- and GDP-bound forms. Similar to the case of HypB, GTP-binding induces dimerization of HypA/B complex, presumably through dimerization of HypB. However, dimerization of HypA/B complex is much weaker than that of HypB, suggesting that interaction with HypA will weaken the HypB dimerization.

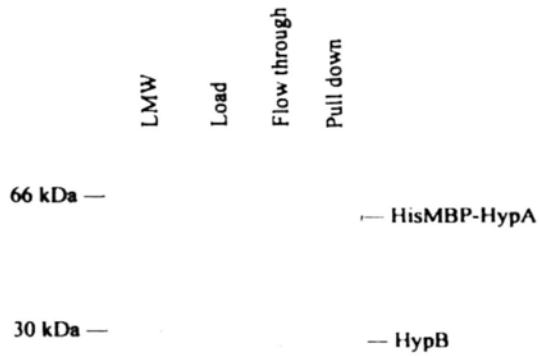

Figure 4.1 HypB interacts with HypA by pull-down assay. HypA fused to HisMBP-tag was immobilized on an amlyose agarose column pre-equilibrated with binding buffer. HypB was loaded onto the immobilized column. After extensive washing, the binding complex was eluted with maltose and analyzed by 12.5% SDS-PAGE with Coomassie blue staining.

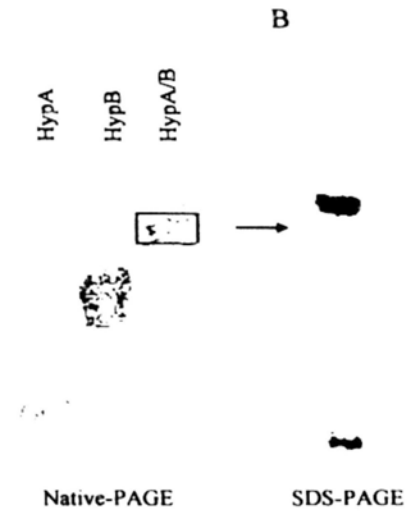

Figure 4.2 Formation of HypA/B complex. HypB was incubated with HypA in 1:1 molar ratio at room temperature. After 15 min incubation, the mixture was analyzed by native-PAGE. (A) Native-PAGE analysis of the mixture of HypA and HypB. An upshift band indicates the HypA/B complex formation. The shifted band was sliced from the gel and subjected to SDS-PAGE analysis. (B) SDS-PAGE analysis of the HypA/B complex. The presence of two dissociated bands corresponds to the HypA and HypB.

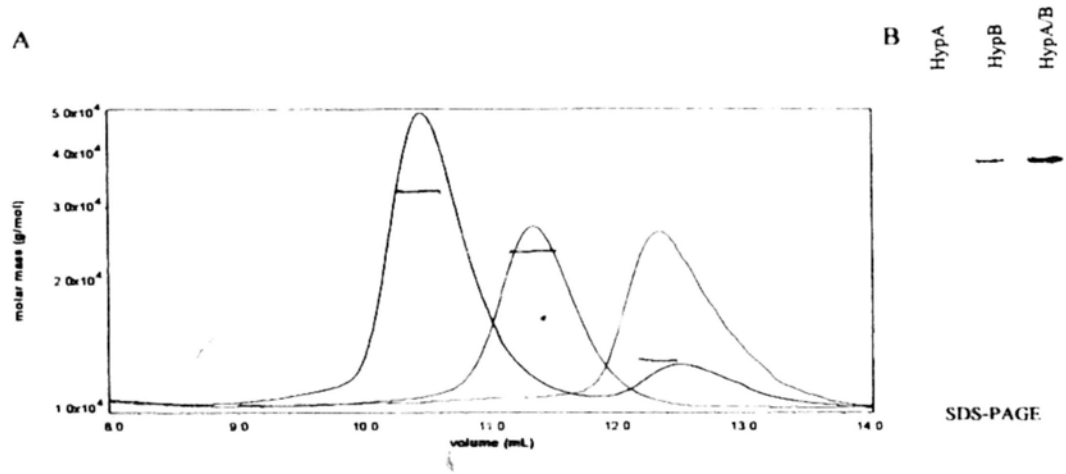

Figure 4.3 Stoichiometry of HypA/B complex is 1:1. The solid lines represent the reflective index measured, which indicates the relative amount of protein pass through the detector. Dots represent the calculated molar mass of fractions pass through the detector. The mixture of purified HypA and HypB was fractionated by Superdex™ 75 column pre-equilibrated with HEPES buffer. The molecular weight of HypA/B dominant species (black line) was found to be 37 kDa. Since the monomeric molecular weight of HypA (red line) and HypB (blue line) are 12 kDa and 25 kDa respectively, thus HypA/B complex is formed by HypA and HypB in 1:1 molar ratio. Fractions from each dominant peak were collected and subjected to SDS-PAGE analysis.

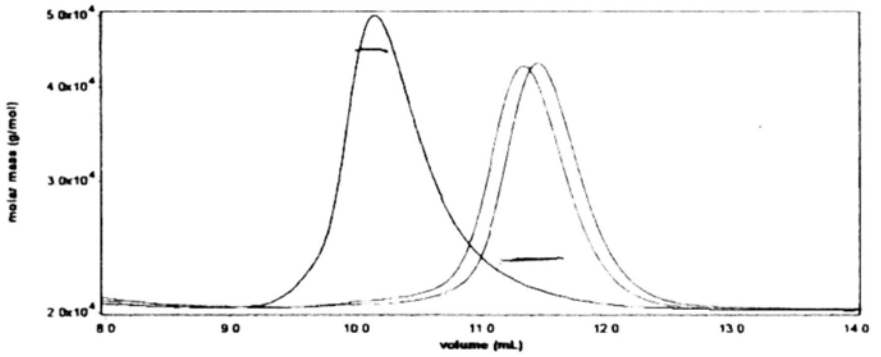

Figure 4.4 HypB dimerizes upon GMPPNP binding. The solid line indicates reflective index trace of HypB in the absence and presence of equal-molar GDP or GMPPNP. The average molar weight of apo-HypB was found to be 24 kDa (red line), that of HypB bound with GDP was also 24 kDa (blue line) and that of HypB bound with GMPPNP was 47 kDa (black line). Theoretical molecular weight of HypB should be 25 kDa. So HypB exists as a monomer in apo- and GDP-bound form, whereas forms a homodimer in GTP-bound form.

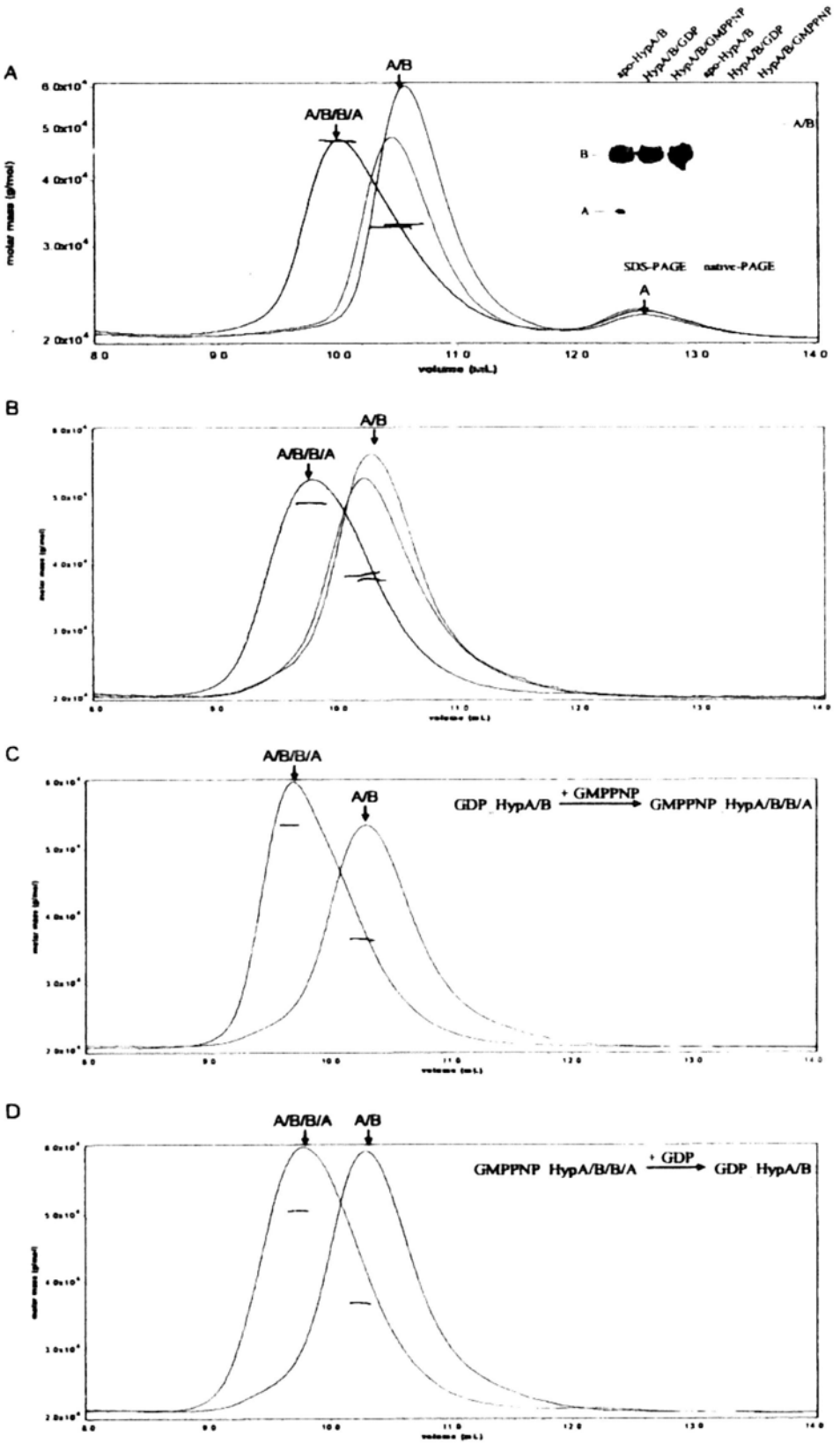
A
B
C
D
A/B
A/B/B/A
apo-HypA/B
HypA/B/GDP
HypA/B/GMPPNP
SDS-PAGE
native-PAGE
GDP HypA/B + GMPPNP GMPPNP HypA/B/B/A
GMPPNP HypA/B/B/A + GDP GDP HypA/B

Figure 4.5

Figure 4.5 HypA/B complexes in apo-, GDP-bound and GTP-bound forms. (A) The mixture of 150 μM HypA and 100 μM HypB was pre-incubated with 200 μM GDP or GMPPNP prior to loading to the Superdex™ 75 10/300 GL column. HypB formed a hetero-dimer with HypA in apo-form (red line) or GDP-bound form (blue line) with a molecular weight of 34 kDa each. The mixture of HypA and HypB in the presence of GMPPNP (black line) gave rise to a species with a molecular mass of 49 kDa. SDS-PAGE and native-PAGE analysis of this species showed the presence of HypA and HypB and homogeneous as well. (B) The 100 μM purified HypA/B complex was pre-incubated with 200 μM GDP or GMPPNP prior to loading to the column. The molecular weight of HypA/B complex in apo-form (red line) and GDP-bound form (blue line) are 37 kDa and 38 kDa respectively, indicative of the formation of hetero-dimer. The molecular weight of HypA/B complex in the presence of GMPPNP is 49 kDa (black line). Since the complex of 49 kDa was eluted earlier than the hetero-dimeric HypA/B complex and no any portion was dissociated from the complex. So the stoichiometry of GMPPNP-bound HypA/B complex is a hetero-tetramer of HypA/B/B/A. (C) The conversion of HypA/B from GDP-bound form to GTP-bound form. The 100 μM purified HypA/B complex was pre-incubated with 200 μM GDP prior to load to the column. The elution containing the GDP-bound HypA/B was collect and incubated with 1 mM GMPPNP in large excess. HypA/B in GDP-bound form (red line) formed hetero-dimer with a molecular weight of 37 kDa, whereas it converted to GTP-bound form (blue line) with a molecular weight of 54 kDa by addition of excess GMPPNP. (D) The conversion of HypA/B complex from GTP-bound form to GDP-bound form. HypA/B complex in GTP-bound form (red line) formed hetero-dimer with a molecular weight of 34 kDa, whereas it converted to GDP-bound form (blue line) with a molecular weight of 37 kDa by addition of large excess GDP. Conversion of HypA/B complex between GDP-bound form and GTP-bound form is reversible and during the conversion of GMPPNP-bound HypA/B complex to GDP-bound HypA/B, no protein is dissociated, indicating of the equilibrium between two states.

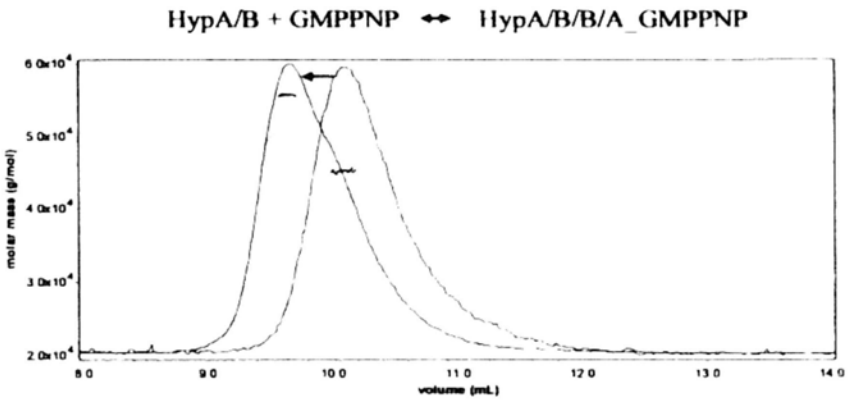

Figure 4.6 Effect of increasing concentration of ligand. The calculated molecular weight of HypA/B complex was 45 kDa in the presence of 100 μM GMPPNP (red line), whereas increased to 56 kDa in the presence of 1 mM GMPPNP (blue line). Since the molecular weight of heterodimeric HypA/B is 37 kDa, HypA/B complex in the presence of GMPPNP exists as the intermediate of the equilibrium between the two states of the apo-HypA/B complex and the GMPPNP-bound HypA/B/B/A complex. The increasing concentration of GMPPNP could propel the equilibrium to the formation of the GMPPNP-bound HypA/B/B/A.

Table 4.1 Effect of HypA binding on dimerization of HypB with increasing concentrations of GMPPNP.

	[Protein], μM	[GMPPNP], μM	M.W.$_{meas.}$, kDa	M.W.$_{exp.}$, kDa	Dimeric HypB%[a]	K_d, μM[b]
HypB	100	100	47	50	~90	~2
HypA/B	100	100	45	74	~20	~300
		200	50		~35	~100
		1000	56		~50	~50

[a] The percentage of dimerization of HypB is derived from the expected and measured molecular weight. [b] Comparison of the various dissociation constants for the formation of HypB dimer showed HypB dimer were dissociated upon HypA binding to various extent in response to the different concentration of ligand, which indicates the HypA play a role in dissociation of HypB dimer and the dissociation is the GMPPNP-dependent.

Chapter 5

Biological Characteristics of AfHypB

5.1 Introduction

It has been shown that the hydrogenase activity of the hypA and hypB mutants can partially restored by Ni supplementation in the growth media. So both HypA and HypB are essential for nickel incorporation into hydrogenases (Jacobi, Rossmann et al. 1992; Maier, Jacobi et al. 1993). Interaction between AfHypA and AfHypB has been determined by pull-down assay. This finding will help us to find out how the formation of HypA/B complex affects its biological activities.

Prior to investigation on HypA/B complex, the biological functions of HypB including Ni binding ability, the GTPase activity and guanine nucleotide binding should be determined at first. And whether the GTP hydrolysis is coupled to Ni presenting and the role of HypA played in this process will also be discussed.

5.2 Ni binding to HypB

To further understand the function of HypB in the hydrogenase maturation pathway, we investigated its Ni binding properties at first. The Ni binding abilities of the purified HypA and HypB were determined by equilibrium dialysis followed by atomic absorption spectrophotometry. Equilibrium dialysis is a simple but effective tool for the study of interactions between molecules. In a standard equilibrium dialysis assay, there are two chambers separated by a dialysis membrane. A ligand is placed into one of the chambers. As the ligand diffuses across the membrane some of it will bind to the receptor and some will remain free in solution. Diffusion of the ligand across the membrane and binding of the ligand continues until equilibrium has been reached. At equilibrium, the concentration of ligand free in solution is the same in both chambers. The concentration of free ligand in the ligand chamber can then be used to determine the binding affinity of the samples.

5.2.1 Ni binding stoichiometry of HypB

Equilibrium dialysis of 15 μM HypB with $Ni(NO_3)_2$ standard solution diluted with various concentrations was performed in equilibrium dialyzer with precut dialysis membranes (M.W. cutoff = 5000). 5 mM TCEP was present during the experiment to avoid oxidation. After 48 hr incubation at 4 °C, the Ni concentration was measured in aliquots from each compartment by atomic absorption spectrophotometry. The binding curve is plotted by the following equation for fractional saturation (Y):

$$Y = \frac{B_{max} \cdot [Ni^{2+}]}{K_{d(ave)} + [Ni^{2+}]}$$

Where B_{max} is constant reflecting maximal binding, and K_d is the dissociation constant (Lee, Pankratz et al. 1993; Wakabayashi, Schmidt et al. 2002). This equation represents a single-site binding model, which is considering that the metal ions show identical affinities for the different sites, such as homogeneous binding.

It has been demonstrated that HypB dimerized upon GTP-binding, which is in contrast to HypB as a monomer in apo-form and GDP-bound form. But less is known about the Ni binding of HypB upon GDP or GTP-binding. To clarify this question, we tested the Ni binding ability in the presence of GDP or GMPPNP. The results showed that HypB bound 2 Ni ions in the presence of GDP (Fig. 5.1A) and 5 Ni ions in the presence of GMPPNP (Fig. 5.1B). Given that the HypB dimerization upon GTP binding is associated with additional Ni binding, it is possible that the dimer interface is an important position for binding an extra Ni and possesses a possible role in Ni presenting upon GTP hydrolysis.

Based on the stoichiometries of Ni binding to HypB in GDP-bound form and GTP-bound form, it is reasonable to speculate that the formation of HypB dimer upon GTP-binding generates a Ni binding site at the dimer interface, and GTP hydrolysis may initiate some steps to release one Ni to the hydrogenase apoenzyme.

5.2.2 Ni binding sites

5.2.2.1 Prediction of Ni binding sites

A recent investigation shows that HypB from *E. coli* contains two metal-binding sites, one is located at the N-terminal CxxCGC motif and the second is in the G-domain, including residues of Cys166, His167, and Cys198. AfHypB lacks the N-terminal sequences and corresponding N-terminal nickel-binding site. Sequence alignments show that the second nickel-binding site located in the G-domain is completely conserved among members of the HypB family. In AfHypB these conserved residues are located at the 92, 93 and 122 position. In addition, another Ni binding site is observed in the crystal structure of MjHypB. Sequence alignment showed it also existed in AfHypB, which is composed of His97 and His101. But this binding site is not conserved in other members of HypB family (Fig. 5.2A).

The binding site of H97/H101 is exposed to solvent and point away from the dimer interface. H97/H101 and their counterparts in another HypB molecule of the adjacent asymmetric unit constitute the tetragonal histidines coordination. This binding site may function in Ni storage in order to keep the low concentration of free-metal ion in the cytoplasm. The similar binding pattern is also observed in MjHypB.

As shown in figure 5.2, the binding site of C92/H93/C122 is located at the dimer interface, accordingly we speculate that the dimer formation could create an extra Ni-binding site composed of C92/C122 from chain A and their counterparts from chain B. Therefore, three Ni binding sites are symmetrically located in the dimer interface including the two binding sites of C92/H93/C122 in respective chain. However, this putative binding pattern is different to that in Zn-bound MjHypB, where asymmetric Zn coordination is absent in C95/H96/C127 of chain A. One explanation is that His96 forms a tight aromatic stacking interaction with Phe131 but not involved in binding Zn (Gasper, Scrima et al. 2006).

The existence of a bimetallic center asymmetrically coordinated by both monomers

in MjHypB is suspected with the following viewpoints. Firstly, the MjHypB structure showed four Zn ions bound to dimeric HypB, which is inconsistent with our finding that the dimeric HypB in GTP-bound form could bind five Ni^{2+} ions. Secondly, the metal binding model of MjHypB is established by Zn ion. After all, the Ni property is different from that of Zn since the Ni-soaked MjHypB had lower intensity for Ni than for Zn at the site of His100 and His104 (Gasper, Scrima et al. 2006). Furthermore, the Zn occupancy in different coordination is not constant. So it is reasonable to suspect the asymmetric distribution of Zn ions might be a mistake for ignoring the low density of one Zn ion. Therefore, taken together, it is reasonable to assume that the HypB dimer in complex with GTP analogue could bind three Ni ions symmetrically within the interface of C92/H93/C122 cluster.

Based on the above statements, we suggest the following hypothesis. HypB is a GTP-dependant maturation factor for delivery Ni to the active site of the hydrogenase. It is dimerized in the presence of GTP and bound one more Ni at the dimer interface mediated by GTP. When GTP hydrolyzed, the Ni trapped in this site is released and incorporated to the metallocenter of hydrogenase. So the Ni processing by HypB is dimer-mediated and GTP-dependant. But whether the putative Ni binding sites is corrected, site-directed mutations would be introduced to verify this binding site.

5.2.2.2 Mutagenesis of Ni binding sites

Sequence alignment showed five residues, including Cys92, His93, Cys122, His97 and His101, are involved to constitute two Ni binding sites. To locate the Ni binding sites, site-directed mutations were introduced by substitution of the residues with non-ligand alanine. Therefore, the C92A/C122A and H97A/H101A variants were constructed. Multiple-alanine mutants of these residues involved in Ni binding were expressed and purified. The Ni-binding ability of each variant was investigated by equilibrium dialysis in the same manner as HypB wild-type.

5.2.2.3 Determination of Ni binding sites

Equilibrium dialysis demonstrated the following mutation-function correlation: substitution of Cys with Ala abolished the C92/H93/C122 Ni binding site, while substitution of His with Ala abolished the H97/H101 binding site. Therefore, both motifs are required for Ni binding. The Ni binding stoichiometry of HypB wild type is almost identical to the stoichiometry summation of Ni binding to C92A/C122A and H97A/H101A. The Ni binding stoichiometries for the HypB and its variants is summarized in Table 5.1.

It is noteworthy that the H97A/H101A variant could bind one and three Ni ions in the presence of GDP and GMPPNP respectively (Fig. 5.3A), while the C92A/C122A variant could bind one Ni ion in the presence of GDP and GMPPNP (Fig. 5.3B). The fact that dimeric H97A/H101A could bind 3 Ni ions in the presence of GMPPNP indicates the significant role played by the Ni binding site composed of C92/H93/C122 in specific Ni binding. And this specific Ni may be released via the GTP hydrolysis of HypB. In addition, sequence alignment showed that the motif of C92/H93/C122 is well conserved among other HypB proteins compared to H97/H101 motif. From these results we could conclude that the C92/H93/C122 binding site is more essential for Ni incorporation into the hydrogenase active site.

Furthermore, the Ni binding site of H97/H101 is located in the internal molecule, while the other Ni binding site of C92/H93/C122 is located at the interface of the dimeric molecules. In the presence of GMPPNP the H97A/H101A variant retained the same the Ni binding pattern as HypB wild type with an extra Ni bound, other than C92A/C122A variant. These results raised a possibility that an extra Ni ion was coordinated by two Cys92 and two Cys122 supplied by dimeric HypB in GTP-bound form, which is support by that fact that a dimeric form of the MjHypB was detected in crystal with two monomers bridged by a Ni bound to four cysteines ligands provided by each monomer.

In addition, it is interesting to note that the two Ni binding sites possess the

different affinities in micromolar range. The composited K_d for wild type or H97A/H101A variant in dimeric GTP-bound form is higher than its monomeric GDP-bound form (Table 5.1). So the Ni binding site at the dimer interface formed by Cys92 and Cys122 has a higher K_d than that of C92/H93/C122 and H97/H101 binding sites in each molecule. It is likely that the lower affinity of this intermolecular binding site indicates that it is easier to release Ni to hydrogenase precursor upon the GTP hydrolysis.

5.2.3 Ni-induced dimerization of HypB

5.2.3.1 Preparation of oxidized and reduced HypB

The free thiolates content of HypB was determined by the method of Ellman (Ellman 1959). Briefly, protein as added to a 1 mM DTNB solution in 20 mM Tris, pH 8.0, and 100 mM NaCl, to final concentration of 10 mM. After incubation for 10 min at 37 °C, the amount of generated *p*-nitrothiolate was determined using the molar absorption coefficient (ε412) of 13600 $M^{-1}cm^{-1}$.

The oxidized HypB is available when the purification procedures are carried out in air without the protection of the reducing agents. The purified HypB are generally >90% oxidized and a disulfide bound is present without the protection of reducing agent. After treatment with TCEP, the free thiols could be recovered nearly 100%.

5.2.3.2 Reduced HypB dimerizes upon Ni-binding

HypB in oxidized or reduced form is prepared in the absence and presence of excess TCEP as a reducing agent. As shown in figure 5.4, in the presence of Ni, HypB purified under the condition without protection of reducing agent only yielded a single peak, corresponding to a monomeric HypB. However, the HypB incubated with TCEP yielded additional peak with earlier elution time. The experiments described here establish a strong correlation between Ni binding and Ni-coupled dimerization, suggesting that the Ni plays a role in dimerization of HypB. But the physiological role of the Ni-induced dimerization has not been demonstrated yet.

In addition, even if the column buffer is absence of Ni, the Ni-containing HypB did not dissociated into monomer upon dilution into the Ni-free solution while migrating in the column. This suggested that the Ni-binding would be so tightly that the bound Ni was not release during migration.

There are three cysteines existed in the HypB, among of which two cysteines of Cys92 and Cys122 are so close in the space as to form disulfide bond when oxidized. The formation of disulfide bond is associated with incapability of dimerization in the presence of Ni. So it is possible that two cysteine residues are involved in Ni binding.

5.2.3.3 Ni-induced dimerization is a reversible process

To investigate whether the Ni-induced dimerization is a reversible process, we performed the following experiments. The results obtained by SEC/LS are shown in figure 5.5.

The experiment initiated with the determination of the reduced HypB conformation, which exhibited a monomer. After then, Ni was added to HypB. The protein was capable of dimerization in complex with Ni. The presence of dimeric Ni-bound HypB in reduced form is dominant, whereas the monomeric HypB in oxidized form represents only a minor fraction. Dimeric Ni-bound HypB was purified by analytical gel filtration to obtain a single peak composed of fully reduced HypB.

The bound-Ni could be removed from HypB by incubation with 10 mM EDTA for overnight at 4 °C followed by dialysis against Ni-free buffer. This process converted the dimeric Ni-bound HypB to the monomeric apo-HypB form. Due to the incompletely dialysis, a little Ni left in HypB solution results in the observation of a minor portion of dimeric Ni-bound HypB.

Re-loading of Ni to the apo-HypB prepared in the same manner yielded a dimeric

Ni-bound form again. A little portion of oxidized HypB was observed, probably due to the rapid oxidation of the apo-HypB cysteine during the dialysis for recovering Ni-bound HypB to the apo-form.

Taken together, cysteine oxidation disrupted the Ni binding and significantly impaired the HypB dimerization. In contrast, reduction of oxidized form with TCEP could recover the Ni binding ability, demonstrating that the Ni binding situation was functional convertibility.

5.2.3.4 Ni-bound HypB remains in dimeric form when interacted with G-nucleotide

As mentioned above, the reduced HypB exists as a dimer in the presence of Ni. It is interesting to note that dimerization could also be occurred in GDP-bound form or GTP-bound form of HypB in the presence of Ni ion (Fig. 5.6). Since these HypB forms are all present as dimeric form in the gel filtration buffer containing Ni, it is possible that HypB may exhibit the function as a dimer involved in the Ni incorporation pathway. The addition of stoichiometric Ni may have an effect on the stability of HypB in reduced form.

5.2.4 GTP-dependent dimerization is independent of Ni-binding

It is reported that the conformational change of HypB upon GTP hydrolysis is responsible for the Ni delivery to the active site of hydrogenase. And the fact that one of the conserved Ni-binding site of C92/H93/C122 overlaps with the GTP-binding site of HypB also implicates the relationship between the Ni-binding and GTP-binding. Therefore, to elucidate whether the Ni binding is required for GTP binding and subsequent GTP-dependent dimerization of HypB, the mutants deficient in the Ni binding ability were investigated to address this question.

The HypB variants of C92A, H93A and H101A were selected for investigation of GTP-dependent dimerization. The Cys92 and His93 are involved in one of the Ni binding sites located at the interface of the two molecules for the HypB dimer. The

H101 is involved in an intra-molecular Ni binding site extruded outside from dimer interface. Equilibrium dialysis showed these variants were all deficient in one of the Ni binding sites.

The HypB variants were subjected to SEC/LS analysis in a similar approach as mentioned previously. The oligomerization was found to be the same as the wild type. As shown in figure 5.7, C92A (3 mg/mL) was found to be a monomer in the presence of 200 μL GDP, but formed dimer when interacted with GMPPNP. So did the mutants of H93A and H101A. These results indicate that the formation of the dimeric GTP-bound HypB does not require the Ni-binding residue, even if the conserved Cys92, His93 is in close proximity with the GTP-binding motif.

From the results, all of these variants could dimerize in the presence of GMPPNP, whereas exist as monomer in the presence of GDP, which indicates that GDP/GTP binding is irrelevant to the Ni binding to HypB and the GTP-induced dimerization is independently of Ni binding.

5.3 HypB is a G-protein0

5.3.1 GTPase activity of HypB

Based on the AfHypB structure, HypB shows the presence of conserved GTP-binding motifs, which are speculated to bind and hydrolyze GTP (Bourne, Sanders et al. 1991). Therefore, purified HypB was assayed for its GTPase activity.

GTP-hydrolysis activity was measured by the colorimetric method with malachite green (Geladopoulos, Sotiroudis et al. 1991; Fisher and Higgins 1994). Figure 5.8 shows a time course of GTPase activity. The released phosphate was measured at different time intervals as indicated on the *x* axis. Analysis of the result indicated that HypB had a GTPase of 0.8 nmol of GTP hydrolyzed per nmol of HypB and the hydrolysis rate was linear over 4 hours.

5.3.2 Nucleotide binding to HypB

Fluorescently labeled nucleotides have been widely used to study the interactions of nucleotide-binding proteins with their substrates. In the case of GTPases the modification of the hydroxyl group of the ribose moiety of GTP with methyl-anthraniloyl (mant-) derivates was used as a tool to determine the nucleotide affinities in various studies. The addition of the mant-group did not severely impair the binding properties of the proteins in GTPases since the hydroxyl moieties of the ribose are mainly solvent exposed.

The affinity of HypB to nucleotide was determined by fluorescence resonance energy transfer (FRET), which is a technique for measuring the interactions between two molecules. In FRET, light energy is added at the excitation frequency for the tryptophan surrounding the binding site of HypB (Hiratsuka 1983), a fluorescent analogue of 5'-GDP, which transfers some of this energy to the mant-GDP, which then re-emits the light at its own emission wavelength. So if the fluorescence intensity increased, there must be an interaction existed between the mant-GDP and HypB.

5.3.2.1 Mg^{2+} as a cofactor for nucleotide binding

As shown in figure 5.9, HypB was titrated with mGDP in the presence and absence of the Mg^{2+} respectively. The fluorescence intensity (Y axis) was monitored at λ_{em} of 450 nm with excitation at λ_{ex} of 295 nm. The basal fluorescence is obtained with mGDP alone as a background. The fluorescence of HypB titrated with mGDP in the absence of Mg^{2+} ion is consistent with the basal fluorescence of mGDP. But the fluorescence was stimulated significantly in presence of Mg^{2+} ion. These results suggest that the mGDP is incapable of binding HypB in the absence of Mg^{2+} ion. That is Mg^{2+} ion serves as the cofactor for nucleotide binding to HypB.

5.3.2.2 K_d of HypB to mGDP

Dissociation constant (K_d) means the total substrate concentration when the protein is 50% bound. It is useful to describe the binding affinity between protein and its substrate. It follows that the smaller K_d, the stronger the binding.

Binding of fluorescent mGDP to HypB was investigated through FRET between the mGDP and the tryptophans of HypB. A 2-ml sample was placed in a temperature-controlled (20 °C) sample holder and the fluorescence of mGDP was monitored at 440 nm. For the fluorescence titrations, the mGDP was added from a 1 mM stock solution to 0.3 μM HypB.

The binding affinity of HypB for the mGDP was measured by titration, as shown in figure 5.10A. The titration was performed in the absence (background fluorescence of mant-nucleotide) or presence of 0.3 μM HypB in the buffer containing 50 mM HEPES, pH 6.8, 0.2 M NaCl, 5 mM $MgCl_2$ respectively. The absolute fluorescence intensity showed in *Y*-axis was background fluorescence of mGDP subtracted from the fluorescence in the presence of HypB measured above. The apparent K_d was determined by fitting the data to a binding equation as described in Chapter 2, which calculated was 0.11 μM.

5.3.2.3 K_i of HypB to GDP

The K_i value for nucleotide was measured indirectly by competition with mGDP. Titration of mGDP binding to HypB was performed as described above in the presence of various concentrations of nucleotide. The apparent K_d values for mGDP were plotted as a function of the nucleotide concentrations. In case of competitive inhibition, the apparent K_d would increase with increasing inhibitor concentration. The K_i value is obtained from negative *X*-intercept of a linear plot.

In a competitive binding experiment, HypB was titrated with mGDP in the presence of increasing amounts of GDP. The K_i for GDP estimated in this way was 0.26 μM (Fig. 5.11A), which is consistent with the K_d for mGDP. It is demonstrated that the mant-group attached to the guanine nucleotide does not interfere with binding.

5.3.2.4 K_i of HypB to GMPPNP

HypB (0.3uM) was titrated with mGDP in the presence of various concentrations of

GMPPNP (0.0625, 0.125, 0.25and 0.5 μM) as competitive inhibitor. The apparent K_d values for mGDP obtained from the titrations were plotted versus the respective GMPPNP concentrations. A linear curve was obtained. The K_i value for GMPPNP given by the *X*-intercept was 1.76 μM (Fig. 5.12A).

5.3.2.5 K_i of HypB to GTP-γ-S GTP-γ

In a competitive binding experiment, HypB was titrated with mGDP in the presence of increasing amounts of GTP-γ-S. The K_i for GTP-γ-S estimated in the same way was 1.07 μM, which is in agreement with the K_i for GMPPNP to HypB (Fig. 5.13A).

5.3.3 Effect of HypA-HypB interaction on nucleotide binding/hydrolysis of HypB

The interaction of HypA and HypB has been identified by pull-down assay, but whether the interaction plays a role in the assembly of the active site of the hydrogenase is not known. So the effect of HypA-HypB interaction will be initiated from the study of GTPase activity and G-nucleotide binding.

5.3.3.1 GTPase activity of HypA/B complex

The previous work showed the intrinsic GTPase activity of HypB was very low, which suggests that HypB is in an "off" state. The GTPase activity might be dependent upon its interaction with other proteins acting as GAPs. To test the effect of its interaction with HypA on the GTPase activity of HypB, the GTPase activities of HypA and HypA/B complex were needed to investigate.

Unlike the HypB, the HypA showed negligible GTPase activity. The GTPase activity of HypA/B complex was increased up to 1.2 nmol of GTP hydrolyzed per nmol of HypB within 4 hours. Even then, the intrinsic GTP hydrolysis reaction is still very slow, which is consistent with HypB from *E. coli* (k_{cat} = 0.17 min^{-1} and K_m = 4 μM). No accelerating factor has been described so far.

Although the GTPase activity of HypB could be activated by HypA, the order of magnitude of GTPase activity stimulated by HypA is not large enough to convert HypB to "on" state.

5.3.3.2 K_i of HypA/B complex to GDP or GMPPNP

After confirmed the GTPase activity of HypA/B complex, the effect of HypA-HypB interaction on nucleotide binding of HypB is also investigated.

As summarized in the Table 5.2, the K_d va[illegible] of HypA/B complex to GDP, GMPPNP and GTP-γ-S were measured by competition with mGDP. Taken together, the interaction of HypA and HypB could increase the binding affinity of HypB to GTP analogue slightly but decrease it to GDP analogue simultaneously.

5.3.4 The Ni binding effect on nucleotide binding to HypB

The crystal structure of AfHypB shows that the metal-binding residues are near to the GTPase active site, which suggests a possibility that metal binding may be relevant to GTP hydrolysis. It is generally accepted that GTP hydrolysis by HypB is essential to the Ni insertion to the active site of hydrogenases. But in contrast, whether the Ni bound to AfHypB affects the GTP hydrolysis and the guanine nucleotide binding of HypB is not known. To make it clear, we propose to do the following experiments. The binding affinity of HypB and HypA/B complex to various nucleotides in the presence of Ni is summarized in Table 5.3.

5.3.4.1 The compatible binding for Ni and GDP

As shown in figure 5.11B, we observed a linear relationship between the concentration of GDP competitor rise and the corresponding apparent K_d increasing in the presence of Ni.

The K_i value for GDP in the presence of Ni estimated was 0.27 μM, which is similar to the K_i for GDP of 0.26 μM in the absence of Ni. It is demonstrated that the Ni bound to HypB does not affect the GDP binding to HypB. That is the Ni

binding is compatible with GDP binding to monomeric HypB in GDP-bound form.

5.3.4.2 The incompatible binding for Ni and GMPPNP

In contrast to a linear relationship between the concentration of GMPPNP competitor rise and the corresponding apparent K_d increasing in the absence of Ni (Fig. 5.12A), upon mixing HypB with an assay buffer containing 5 mM Ni, the apparent K_d didn't increase progressively as the GMPPNP competitor concentration increased. Thus, the K_i of GMPPNP derived from the value of negative X-intercept could not be obtained. Similar situation was also observed in the HypA/B complex interacted with GMPPNP in the presence of Ni (Fig. 5.12B).

In correspondence with the GMPPNP competition in the presence of Ni, interaction of HypB with mant-GMPPNP in the absence of Ni significantly enhance the fluorescence of mGMPPNP alone, but in the presence of Ni, the fluorescence of the HypB by addition of mGMPPNP is almost in agreement with the basal fluorescence of mGMPPNP (Fig. 5.14). This observation indicated that the Ni-bound HypB could not bind GMPPNP any more. Since the formation of HypB/GMPPNP/Ni complex was observed by static light scattering. It appears that binding cooperativity for Ni and GMPPNP is dependent of the order for Ni and GMPPNP binding to HypB.

Noteworthy, we have observed that high concentration of Ni can induce dimerization of HypB, regardless of its GDP/GTP bound states. It could not that the Ni-induced dimerization artificial. But if it really existed, Ni insertion by HypB could be regulated by another mechanism. On the basis of the Ni-induced dimerization, we found that the Ni-bound HypB was unable to bind GMPPNP, whereas the GMPPNP-bound HypB retained the Ni binding ability. It indicates that the GTP incorporation must precede the Ni binding. Otherwise, the dimer is locked by Ni in the dimer interface and the nucleotide binding pocket is buried and inaccessible for GTP. Therefore, if the Ni-induced dimerization is really existed, its importance should be noticeable. For instance, the Ni-bound HypB in GDP-bound

form after Ni delivery could not convert to GTP-bound form directly due to the closed conformation. Oxidation of the HypB is a feasible way to release Ni. Once Ni was released, the dimeric HypB could dissociate and return to the monomeric form, which is in turn involved in the sequential GTP-dependent dimerization and dimer-mediated Ni binding. Whether this structural reorganization is the physiological role is not known yet, although it might suggest a redox-regulated mechanism by which the HypB plays a precise role. And whether disulfide bound formation and the corresponding Ni release is regulatory response will be investigated further.

5.4 Summary

Our results showed that HypB can bind two Ni ions per molecule in apo- and GDP-bound forms. The two Ni binding sites involving C92/H93/C122 and H97/H101 were identified by site-directed mutagenesis. Upon GTP-binding, HypB dimer can bind an extra Ni ion, and we showed that by site-directed mutagenesis that the extra Ni binding site involves the conserved C92/H93/C122 residues, which requires the cysteine residues in their reduced form. We also showed that Ni binding can induce dimerization of HypB.

HypB has a very slow GTP hydrolysis reaction rate. Measured by a FRET assay, HypB has a higher binding affinity for GDP than for GTP. These observations suggest that other protein factors, such as GAP or GEF, may be involved in activation of GTP hydrolysis or release of the bound GDP. Noteworthy, the HypA protein may play a role of GEF for HypB because HypA and HypB interactions could enhance the GTP binding and weaken the GDP binding simultaneously.

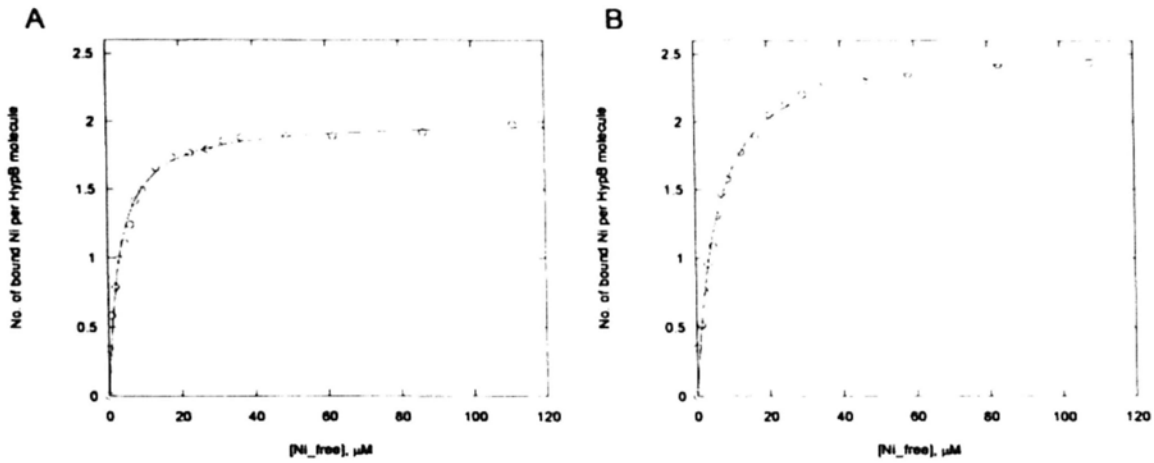

Figure 5.1 Ni binding ability of HypB in GDP-bound form and GTP-bound form. The Ni binding ability of HypB proteins were determined by equilibrium dialysis followed by atomic absorption spectrophotometry. About 14 μM protein was dialyzed against HEPES buffer (pH 6.8) containing increasing concentrations of Ni. Saturation curve is drawn from the curve fit according to a single-site binding model. (A) GDP-bound HypB binds two Ni ions per monomer with a K_d of 3.17 μM. (B) GMPPNP-bound HypB binds 5 Ni ions per homodimer with a K_d of 5.73 μM. That is, the formation of HypB dimer generates an extra Ni binding site at the dimer interface.

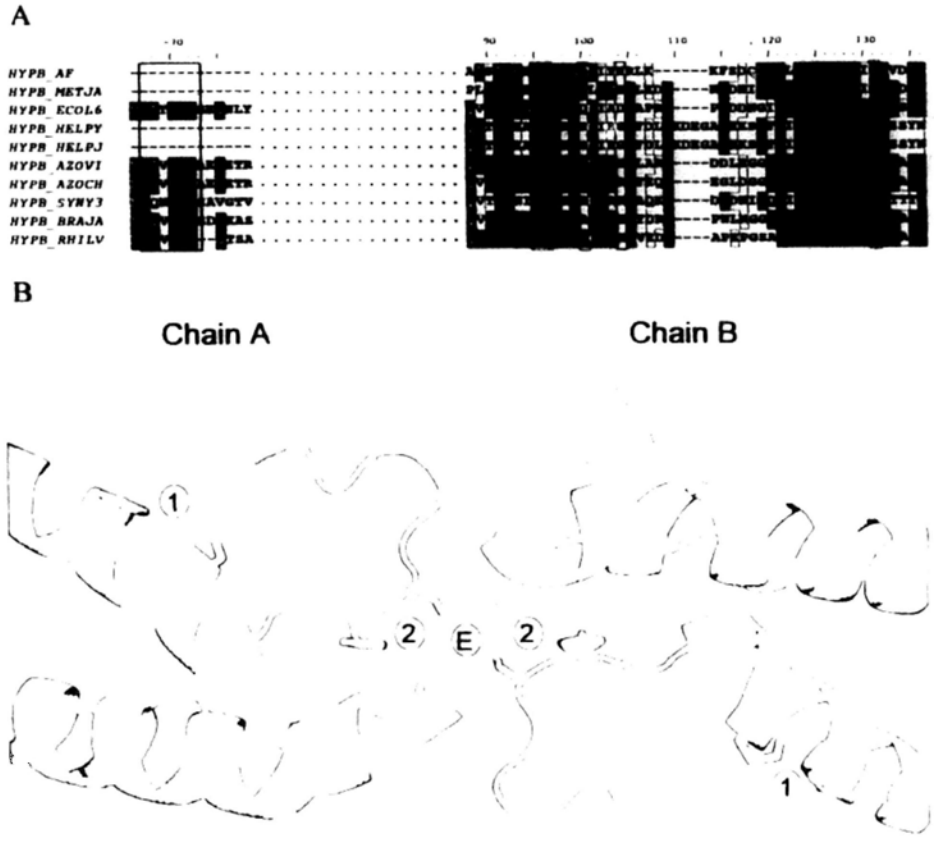
A
HYPB_AF
HYPB_METJA
HYPB_ECOL6
HYPB_HELPY
HYPB_HELPJ
HYPB_AZOVI
HYPB_AZOCH
HYPB_SYNY3
HYPB_BRAJA
HYPB_RHILV
B
Chain A
Chain B
1
2
E
2
1

Figure 5.2

Figure 5.2 The Ni binding sites of HypB. (A) Multiple sequence alignment shows that there are three conserved Ni binding motif in HypB, CxxGCG (blue), CHC (red), HH (green). The CHC motif is conserved in all HypB sequences. AfHypB poses the HH motif but lacks the CxxCGC motif. UniProtKB/Swiss-Prot entry names are indicated on the left. HYPB_AF, *Archaeoglobus fulgidus DSM 4304*; HYPB_METJA, *Methanococcus jannaschii*; HYPB_ECOL6, *Escherichia coli O6*; HYPB_HELPY, *Helicobacter pylori*; HYPB_HELPJ, *Helicobacter pylori J99*; HYPB_AZOVI, *Azotobacter vinelandii*; HYPB_AZOCH, *Azotobacter chroococcum*; HYPB_SYNY3, *Synechocystis sp. strain PCC6803*; HYPB_BRAJA, *Bradyrhizobium japonicum*; HYPB_RHILV, *Rhizobium leguminosarum biovar viciae*. (B) The potential Ni binding sites of AfHypB. The metal ions are shown as pink spheres. Three Ni-binding sites are involved in AfHypB dimer. Ni_1 is coordinated by H97/H101, which is exposed to solvent and points away from the dimer interface. Ni_2 is to be bound by chain B and chain A via C92/H93/C122 respectively. Ni_E is presumed to be coordinated by Cys95 and Cys127 provided by chain A and chain B.

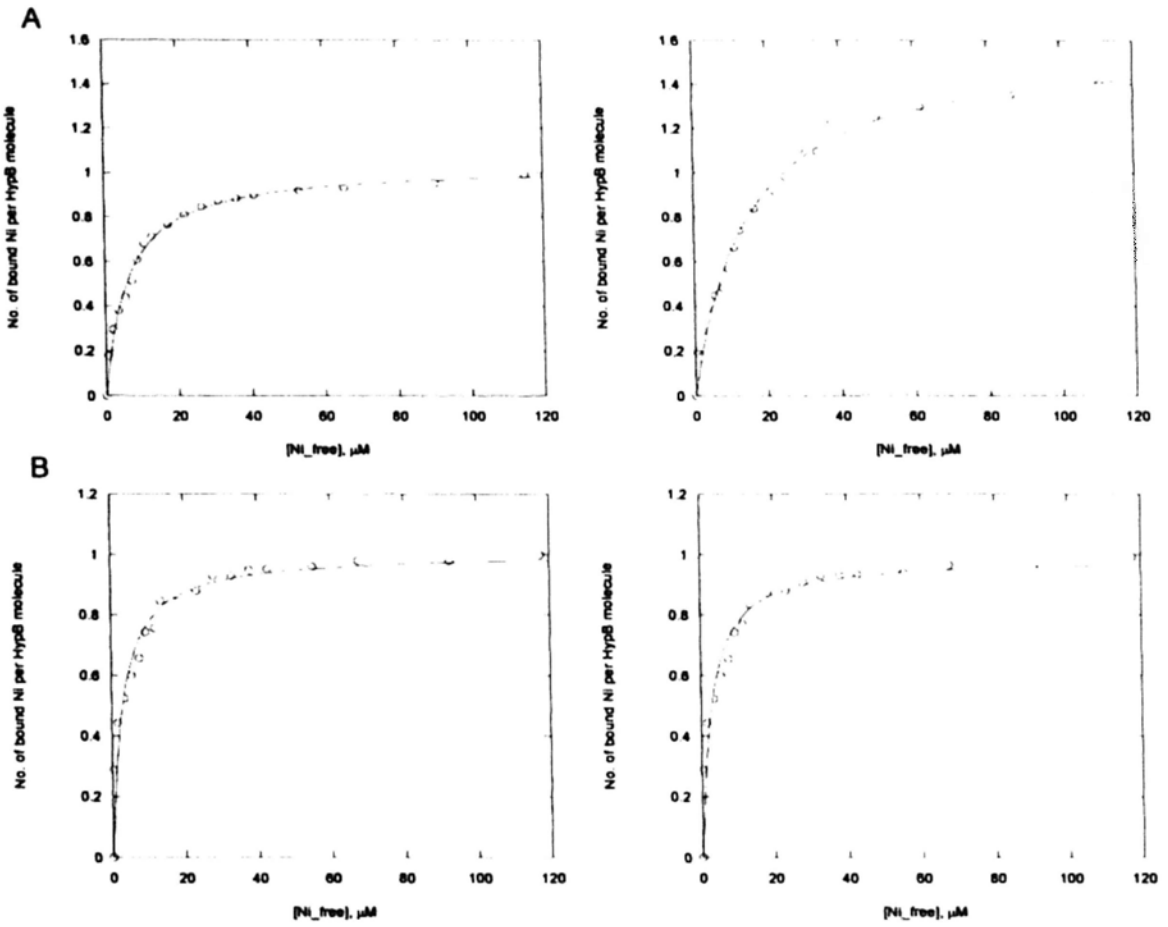

Figure 5.3 Effect of mutating residues involved in Ni binding. The Ni-binding abilities of the HypB mutants (H97A/H101A and C92A/C122A) were determined in the same manner as HypB wild type. Both variants of H97A/H101A and C92A/C122A retained one Ni binding site when disrupted the other one. (A) H97A/H101A variant bound about 1 Ni ion with a less K_d of 6.22 μM in the presence of GDP, while bound about 1.5 Ni ions per monomer with a K_d of 14.79 μM in the presence of GMPPNP. (B) C92A/C122A variant bound about 1 Ni ion with a K_d of 3.0 μM in the presence of GDP, while bound about 1 Ni ion with a K_d of 2.8 μM in the presence of GMPPNP.

Table 5.1 Ni binding characteristics of HypB and its variants

Protein	In GDP-bound form		In GTP-bound form	
	Stoichiometry[a]	K_d, μM	Stoichiometry[a]	K_d, μM
HypB	~2	3.17 ± 0.29	~2.5	5.73 ± 0.42
H97A/H101A	~1	6.22 ± 0.40	~1.5	14.79 ± 1.29
C92A/C122A	~1	3.0 ± 0.43	~1	2.8 ± 0.39

[a]The values are numbers of Ni ions per HypB monomer.

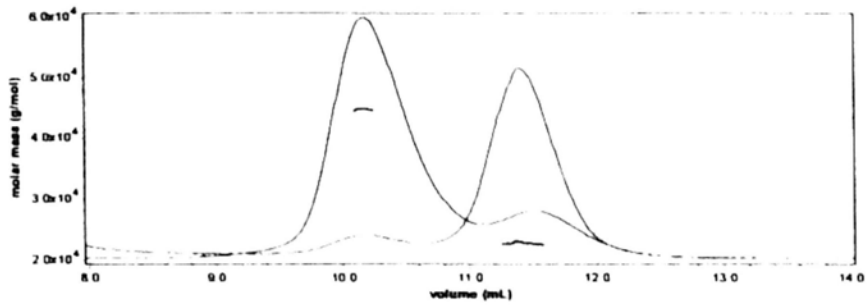

Figure 5.4 Reduced HypB dimerizes upon Ni-binding. The stoichiometry of reduced and oxidized HypB in the presence of Ni was investigated by SEC/LS. The oxidized HypB was achieved when the purification procedures were carried out in air without the protection of reducing agent. The reduced form was derived from the treatment with 5 mM TCEP, a high efficiency reducing agent. The HypB samples (150 μL, 5 mg/mL) were loaded onto the Superdex 75 10/300 GL column equilibrated with the HEPES buffer (pH 6.8) containing 200 mM NaCl, 5 mM $NiSO_4$ and 5 mM $MgCl_2$. The SEC/LS results showed that the Ni-induced dimerization was dominant in the reduced state of HypB (blue line) eluted at 46 kDa, whereas the oxidized state (red line) remained in the monomeric form with a molecular weight of 25 kDa.

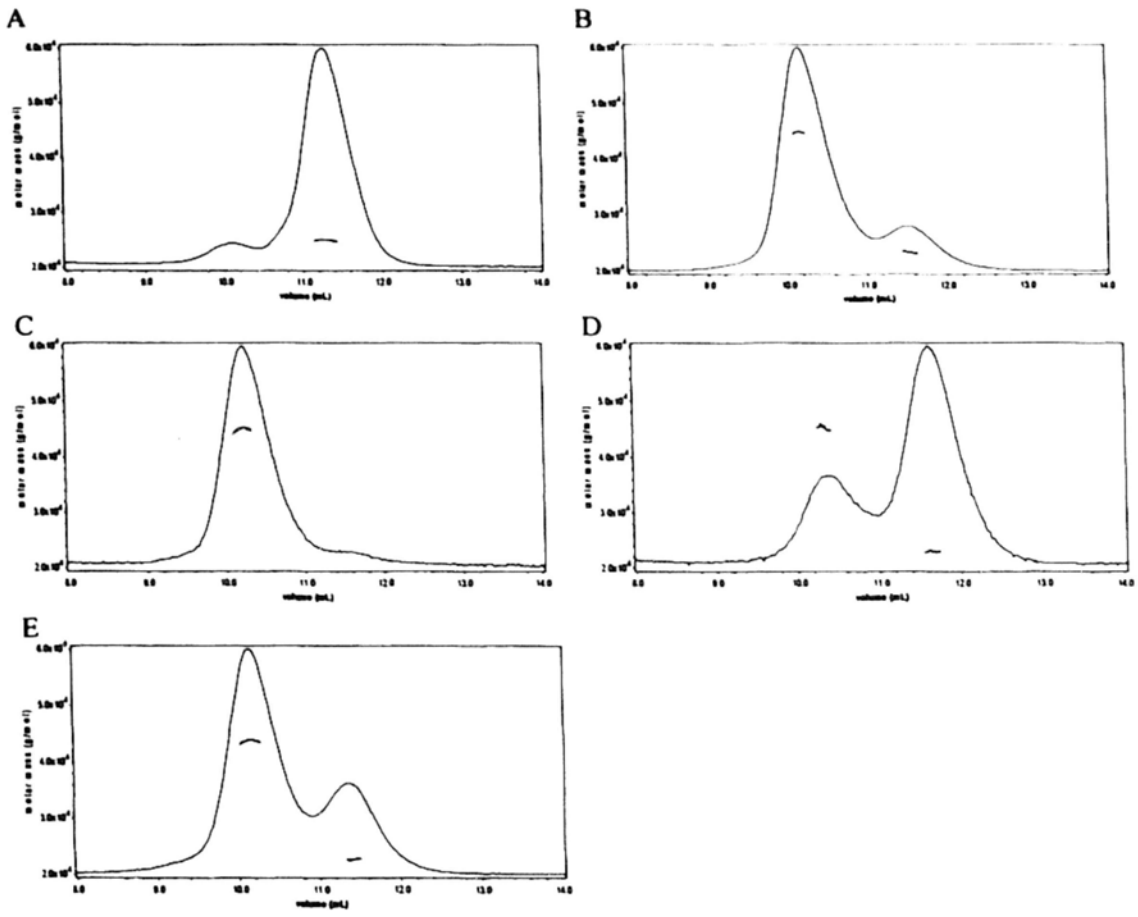

Figure 5.5 Ni-induced dimerization of HypB is reversible. (A) The reduced HypB by treatment with TCEP was eluted as a monomer with a molecular weight of 25 kDa. (B) Major portion of reduced HypB by treatment with TCEP dimerized in the presence of Ni with a molecular weight of 46 kDa. (C) Ni-bound HypB dimer was purified by the Superdex 75 10/300 GL column. The fractions of dimerized HypB was collected and pooled together. (D) The purified Ni-bound HypB dimer dissociated to the monomer with a molecular weight of 23 kDa after removal of Ni by dialysis against the EDTA. (E) The majority of Ni-free HypB is still capable of re-dimerization in the presence of Ni with a molecular weight of 44 kDa. The minor portion with the molecular weight of 23 kDa might be the oxidized HypB derived from the dialysis procedure.

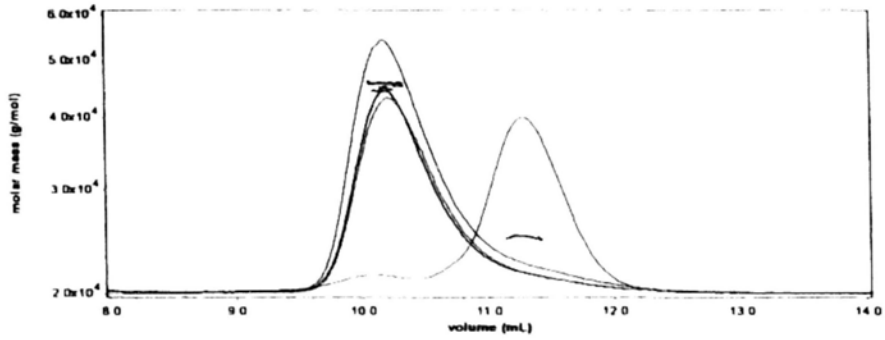

Figure 5.6 Ni-induced dimerization of HypB in apo-form, GDP-bound form and GTP-bound form. The 100 μM reduced HypB was pre-incubated with 200 μM GDP or GMPPNP prior to loading to Superdex 75 column equilibrated with the gel filtration buffer containing 5 mM $NiSO_4$. The reduced-HypB in GDP-bound form (green line) and GTP-bound form (black line) investigated by SEC/LS existed as homodimer in the presence of Ni with a molecular weight of 45 kDa each. That is HypB functions as a dimer when interacted with guanine nucleotide in the presence of Ni, which is consistent with the conformation of reduced HypB (blue line) with a molecular weight of 46 kDa and contrary to that of oxidized HypB (red line) existed as a monomer with a molecular weight of 25 kDa.

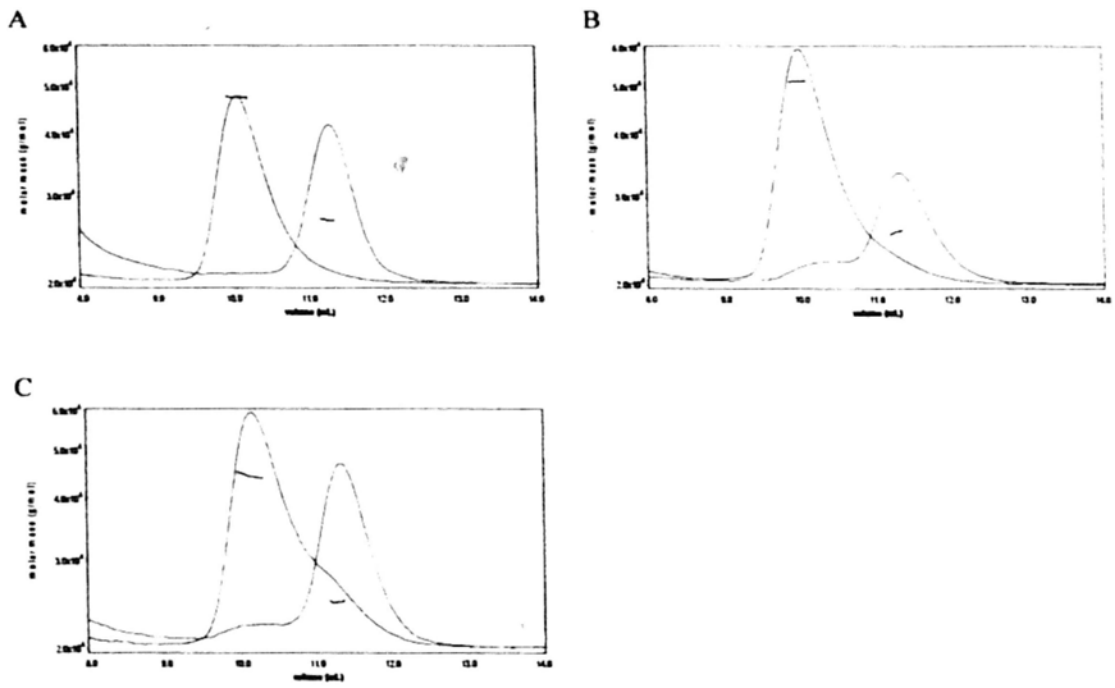

Figure 5.7 GTP-dependent dimerization of HypB is independent of the Ni binding. Mutations were introduced at several residues involved in Ni-binding, Cys92, His93, and His101. Cys92 and His93 are components of the conserved Ni-binding site in the dimer interface. His101 involved in the other binding site points away from the dimer interface. All the variants of C92A, H93A and H101A exhibited a property of GTP-dependent dimerization as the wild type behavior. (A) C92A variant of HypB in the presence of GDP and GMPPNP. C92A variant in GDP-bound form was a monomer with molecular weight of 27 kDa, but formed a homodimer of 50 kDa in the presence of GMPPNP. (B) H93A variant of HypB in the presence of GDP and GMPPNP. H93A variant in GDP-bound form was a monomer with molecular weight of 26 kDa, but formed a homodimer of 53 kDa in the presence of GMPPNP. (C) H101A variant of HypB in the presence of GDP and GMPPNP. H101A variant in GDP-bound form was a monomer with molecular weight of 25 kDa, but formed a homodimer of 47 kDa in the presence of GMPPNP.

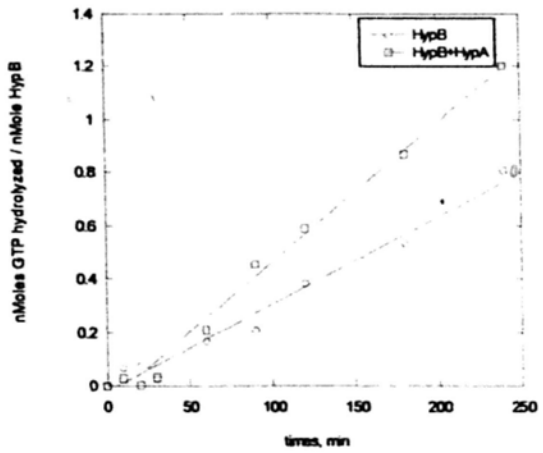

Figure 5.8 GTPase activity of HypB and HypA/B complex. The GTPase activity was measured using the colorimetric method with malachite green. 10 μM enzyme and 20 μM substrate of GTP were used for this assay. The PO_4^{3-} released was measured at different time intervals as indicated on the *x* axis. The HypB showed the GTPase activity of approximate 0.2 nmol of GTP hydrolyzed per nmol of HypB per hour (red line). The HypA/B complex was also tested in the same manner. The activity of HypB could be stimulated a little in the presence of HypA (blue line).

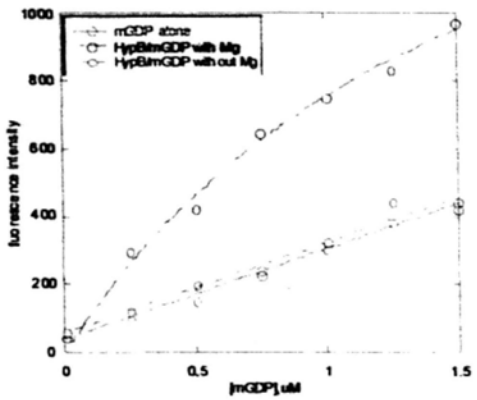

Figure 5.9 Mg^{2+} serves as a cofactor for nucleotide binding to HypB. HypB was titrated with mGDP in the presence and absence of the Mg^{2+} respectively. The basal fluorescence is obtained with mGDP alone as a background (red line). The fluorescence of HypB titrated with mGDP in the absence of Mg^{2+} ion (blue line) is consistent with the basal fluorescence of mGDP. But in presence of Mg^{2+} ion, the fluorescence was increased significantly (black line).

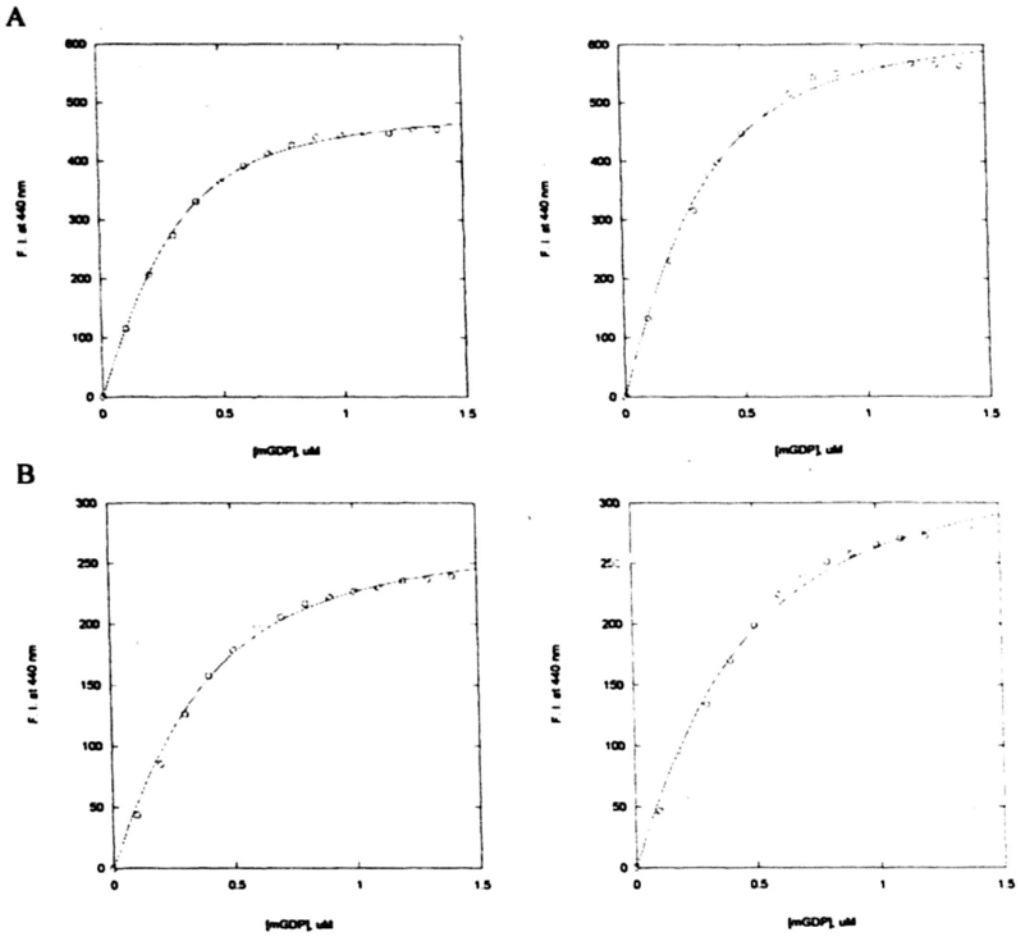

Figure 5.10 Titration curves of HypB and HypA/B complex with mant-GDP in the absence or presence of Ni. Data obtained from the experiments were fit to the binding equation to calculate K_d. (A) Titration curves of HypB and HypA/B complex with mGDP in the absence of Ni. A K_d of 0.11 μM was obtained for mGDP by titration of HypB with mGDP, while a K_d of 0.14 μM was obtained for mGDP by titration of HypA/B complex with mGDP. (B) Titration curves of HypB and HypA/B complex with mGDP in the presence of Ni. A K_d of 0.19 μM was obtained for mGDP by titration of HypB with mGDP, while a K_d of 0.26 μM was obtained for mGDP by titration of HypA/B complex with mGDP in the presence of Ni.

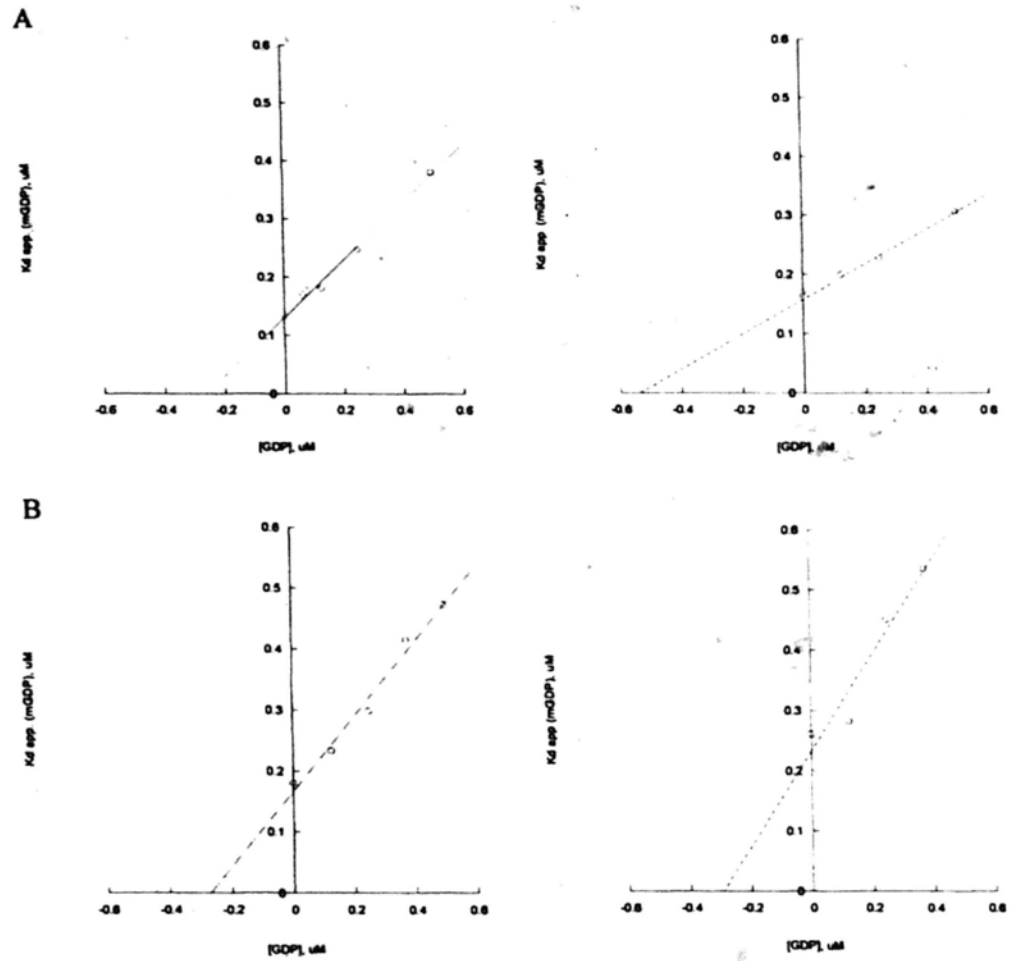

Figure 5.11 Competition of mGDP by GDP in the absence or presence of Ni. (A) Competition of mGDP bound to HypB or HypA/B complex by GDP in the absence of Ni. Protein was titrated with mGDP in the absence or presence of various concentrations of GDP as competitive inhibitor. The apparent K_d values for mGDP obtained from the titrations were plotted versus the respective GDP concentrations. The K_i value for GDP bound to HypB given by the *X*-intercept is 0.26 μM, while the K_i value for GDP bound to HypA/B is 0.54 μM. (B) Competition of mGDP bound to HypB or HypA/B complex by GDP in the presence of Ni. The K_i value for GDP bound to HypB given by the *X*-intercept is 0.27 μM, while the K_i value for GDP bound to HypA/B is 0.29 μM in the presence of Ni.

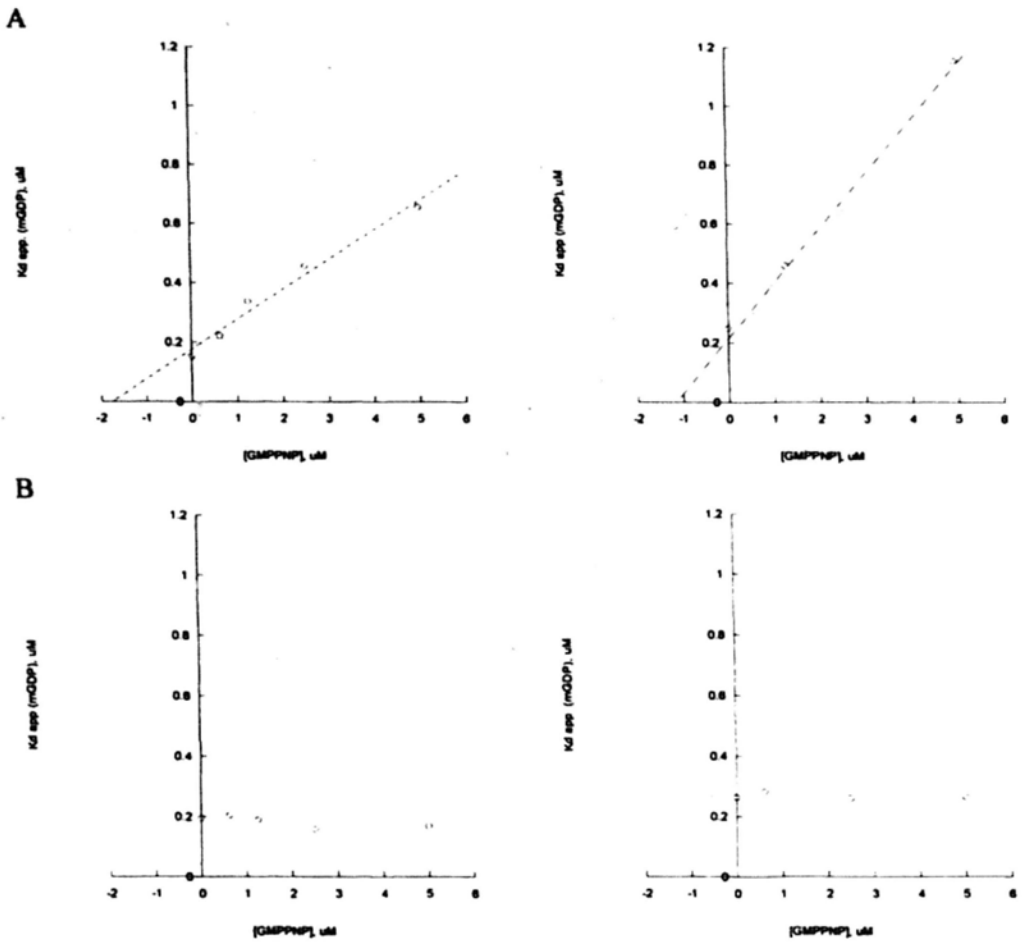

Figure 5.12 Competition of mGDP by GMPPNP in the absence or presence of Ni. (A) Competition of mGDP bound to HypB or HypA/B complex by GMPPNP in the absence of Ni. Protein was titrated with mGDP in the absence or presence of various concentrations of GMPPNP as competitive inhibitor. The apparent K_d values for mGDP obtained from the titrations were plotted versus the respective GMPPNP concentrations. The K_i value for GMPPNP bound to HypB given by the *X*-intercept is 1.76 μM, while the K_i value for GMPPNP bound to HypA/B complex is 1.16 μM. (B) Competition of mGDP bound to HypB or HypA/B complex by GMPPNP in the presence of Ni. It is noteworthy that the apparent K_d didn't increase progressively as the GMPPNP competitor concentration increased, so the K_i derived from the *X*-intercept could not be obtained.

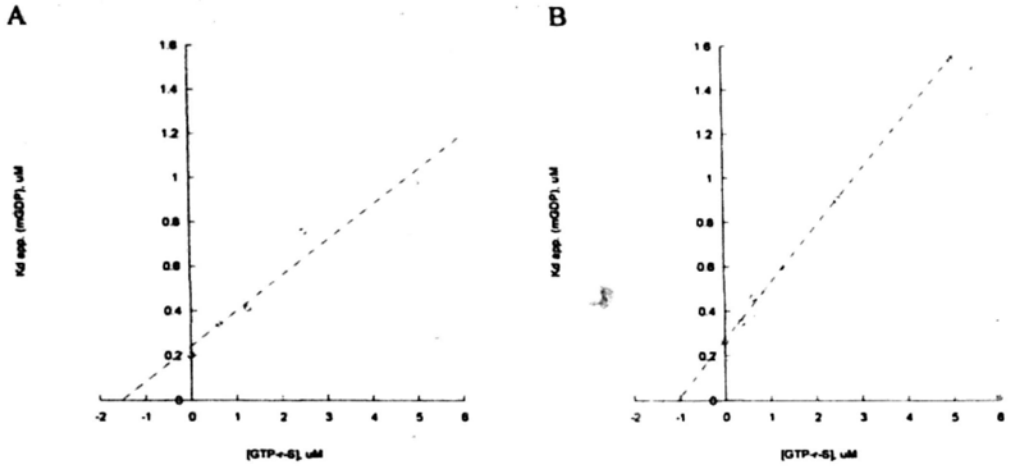

Figure 5.13 Competition of mGDP by GTP-γ-S. (A) Competition of mGDP bound to HypB by GTP-γ-S. HypB was titrated with mGDP in the absence or presence of various concentrations of GTP-γ-S (0.0625, 0.125, 0.25and 0.5 μM) as competitive inhibitor. The apparent K_d values for mGDP obtained from the titrations were plotted versus the respective GTP-γ-S concentrations. The K_i value for GTP-γ-S bound to HypB given by the *X*-intercept is 1.52 μM. (B) Competition of mGDP bound to HypA/B complex by GTP-γ-S. HypA/B complex was titrated with mGDP in the absence or presence of various concentrations of GTP-γ-S (0.0625, 0.125, 0.25 and 0.5 μM) as competitive inhibitor. The K_i value for GTP-γ-S bound to HypA/B complex is 1.07 μM.

Table 5.2 Binding affinity of HypB and HypA/B complex to nucleotide nucleotides in the absence of Ni

	K_d / K_i, μM			
	mGDP	GDP	GMPPNP	GTP-γ-S
apo-HypB	0.11 ± 0.006	0.26 ± 0.018	1.76 ± 0.266	1.52 ± 0.387
apo-HypA/B	0.14 ± 0.015	0.54 ± 0.069	1.16 ± 0.142	1.07 ± 0.045

Table 5.3 Binding affinity of HypB and HypA/B complex to guanine nucleotides in the presence of Ni

	K_d / K_i, μM		
	mGDP	GDP	GMPPNP
apo-HypB	0.19 ± 0.019	0.27 ± 0.032	ND
apo-HypA/B	0.26 ± 0.030	0.29 ± 0.073	ND

ND indicates that binding was tested but was not detected.

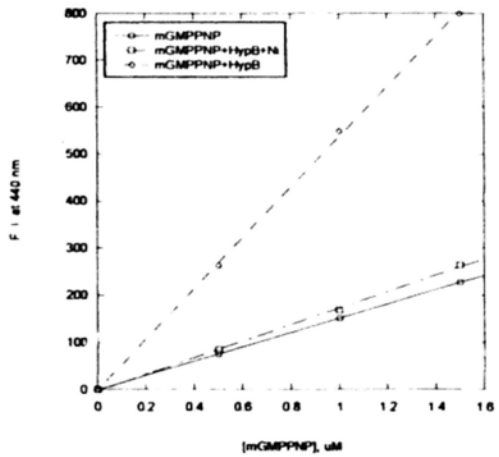

Figure 5.14 Titration of HypB with mant-GMPPNP in the absence or presence of Ni. The basal fluorescence is obtained with mGMPPNP alone as a background (red line). The fluorescence of HypB titrated with mGMPPNP in the presence of Ni^{2+} ion is consistent with the basal fluorescence (blue line). But in absence of Ni^{2+} ion, the fluorescence was increased significantly (green line).

Chapter 6

Discussion

6.1 What do we know so far on the role of HypB in Ni insertion?

6.1.1 How GTP binding lead to dimerization of HypB?

The only structural changes observed between apo-AfHypB and GTP-γ-S-MjHypB are localized in the switch I loop and helix-3 (Fig. 3.4). We have modelled the strucutre of GTP-bound form of AfHypB by modelling the structure of the switch I loop and helix-3 based on those from GTP-γ-S-MjHypB. Sequence alignment between AfHypB and MjHypB showed that all residues involved in GTP binding and dimerization are conserved (Fig 6.1A).

These conserved residues in our modelled structure of GTP-γ-S-AfHypB are able to form the same interactions found in MjHypB (Fig 6.2B). For example, P-loop is involved in binding the α-, β-phosphates. The g-phosphate interacts with the bound Mg^{2+} ion, which is held by T44, D72 and E115. The guanine base is recognized by forming complementary hydrogen bonds with N162, D194, and L195. As discussed in Chapter 3, AfHypB has a non-canonical NKxA motif. The Asp194 located nearby serves to play the role of the aspartate in the NKxD motif in recognizing the guanine base. The GTP lies at the dimeric interface of HypB, and forms inter-chain salt-bridge or hydrogen bonds with K148, A169 and V170, which help stabilizing the HypB dimer.

In particular, K148 forms an inter-chain salt-bridge with Asp72 of helix-3. Structrual comparison between the apo- and GTP-γ-S bound form of HypB suggests that this salt-bridge will be broken by lost of GTP binding. As discussed in Chapter 3, binding of GTP to HypB induces large conformational changes in the switch I loop and helix-3 (Fig. 3.4). Since there is no structural information of GDP-bound form of HypB, it is not known whether the conformational change occurs during GDP or GTP binding. However, we favor the model that these conformational

changes are induced by GTP binding. The switch I loop is held to the P-loop by a salt-bridge between K43 and D66, which blocks the γ-phosphate binding site of GTP. We take the position that GTP binding breaks this salt-bridge and causes the switch I loop to be pushed away from the P-loop. On the other hand, GDP, without the γ-phosphate, can be docked to the active site of apo-AfHypB without major conformational changes.

Taken together, we proposed that GTP binding induces dimerization of HypB by breaking the salt-bridge between K43 and D66, which causes the switch I loop to be moved away from the P-loop. As a result, the conformational changes remove the steric hinderance that allows helix-8 of chain B to dock to the dimeric interface of HypB. Morover, the Asp72 moves ~6 Å to a position that can form the inter-chain salt-bridge with K148 (Fig. 6.2).

6.1.2 One Ni released during one round of GTP hydrolysis

In Chapter 5, we have shown that there are two Ni binding sites in a monomeric HypB. One is the cluster including C92, H93 and C122, the other is composed of H97 and H101. Upon GTP-dependent dimerization, HypB can bind an extra Ni ion. Our results have shown that the C92/H93/C122 is involved in binding the extra Ni ion, and such binding requires both cysteine residues in the reduced form. The crystal structure of MjHypB showed the Cys92 and Cys122 can form a tetra-thiolate coordination sphere at the dimer interface of HypB, where the extra Ni ion is located at the dimeric interface and is coordinated by Cys92 and Cys122 from each subunit of HypB dimer (Fig. 5.2). The role of the C92/H93/C122 cluster is highlighted with the fact that these residues are absolutely conserved in all HypB proteins. Since the GTP-induced dimerization of HypB is coupled to bind an extra Ni, so HypB could act as a GTP-mediated switch that regulate one Ni release from the GTP-bound form to the GDP-bound form.

The other binding site at H97/H101 is not convered, and probably does not play a vital role in the biological function of HypB. It may play a role in Ni storage, in an analogy of HypB from *B. japonicum*, which has an N-terminal poly-Histidine stretch (Fu, Olson et al. 1995).

6.1.3 Role of HypA/HypB interactions

HypA is not a GAP for HypB - The intrinsic GTPase activity of HypB is very low (Fig. 5.8), suggesting that HypB requires a G-protein activating protein (GAP) to activate its GTPase activitiy. Although HypB can interact with HypA to form 1:1 heterodimer, our data suggests that HypA is not a GAP for HypB.

Although the Ni insertion to hydrogenase precursor via GTP hydrolysis is very important, the nature of this trigger is not yet clear. It could involve the interaction of HypB with HycE, a large subunit of hydrogenase, triggers the conformational change, resulting in GTP hydrolysis. The GTP hydrolysis would dissociate the HypB from the complex after Ni inserted (Maier, Jacobi et al. 1993). Unfortunately,

there is no experimental evidence to support these claims. Another assumption suggested by Gasper group is on the basis of a recent X-ray crystal structure of HypB from *M. jannaschii* (Gasper, Scrima et al. 2006). It shows that the Ni binding site is intimately linked to the GTPase active site, suggesting a possible triggering mechanism whereby Ni binding could stimulate GTP hydrolysis. Their hypothesis is contradictory to our finding that only the switch I loop and Helix-3 undergoes the significant conformational change upon GTP-binding or GTP-hydrolysis. Such conformational change induced the formation or dissociation of HypB dimer. And the switch I loop is far way from the functional Ni binding site. So the Ni binding is not required for the GTP hydrolysis.

HypA may serve as a GEF - In the absence of HypA, HypB binds GDP ~6.5 times stronger than GTP. In the presence of HypA, HypB binds GDP only ~2 times stronger than GTP (Table 5.2). This data suggests that HypA may serve as a guanine-nucleotide exchange factors for HypB so that GDP-bound form of HypB can be recycled to the GTP-bound form (Fig. 6.3).

Interaction with HypA weakens HypB dimerization - Our data showed that interaction with HypA could weaken the dimerization of HypB (Table 4.1), and may play a role in assisting Ni release by inducing dissociation of of HypB dimer.

6.2 Conclusion

Based on what we have found, we proposed a model for Ni presenting by HypB involved in hydrogenase maturation (Fig. 6.3). The key feature in this model is that the GTP-dependent dimerization of HypB is coupled to bind an extra Ni for insertion into hydrogenase. The detailed steps will be illuminated as follows.

(1) HypB binds two Ni ions in the apo- and GDP-bound form. Ni binding also induces dimerization of HypB. Upon GTP binding, HypB can bind an extra Ni ion at the dimeric interface. GTP hydrolysis will release the extra Ni ion, which may be subsequently inserted into hydrogenases during the maturation process.

(2) GTP hydrolysis induces conformational changes of HypB in the switch I loop and helix-3, which dissociate the HypB dimer into the monomeric GDP-bound form.

(3) Interaction with HypA alters the relative binding affinity of GDP vs. GTP, allowing the GDP-bound form of HypB ('off' state) to return back to the GTP-bound form ('on' state).

(4) GTP binding breaks the salt-bridge between K43 and D66, and induce conformational changes in the switch I loop and helix-3, which causes the HypB to form dimer and bind an extra Ni ion. The GTP-bound form of HypB is ready for next round of Ni presenting.

6.3 Prospects

Although our study has clarified several roles of HypA and HypB in Ni presenting, there is a number of unresolved issues to be studied in the future.

1. How HypA affects the guanine-nucleotide binding affinity?
In HypB, the P-loop and the switch I loop is responsible for binding the phosphate groups of GDP and GTP. In fact, we have shown that major structural changes were observed in the switch I loop upon GTP binding. If interaction with HypA affects the conformation in these regions, it may then affect the GDP/GTP binding affinity of HypB. Structure determination of HypA/HypB complex may help to address these questions.

2. Is there any structural differences between the apo and GDP bound form of HypB?
Although we believe that the major conformational changes occur upon GTP binding, a comprehensive understanding of the structural mechanism of GTP-dependent dimerization requires structure determination of the GDP-bound form of HypB.

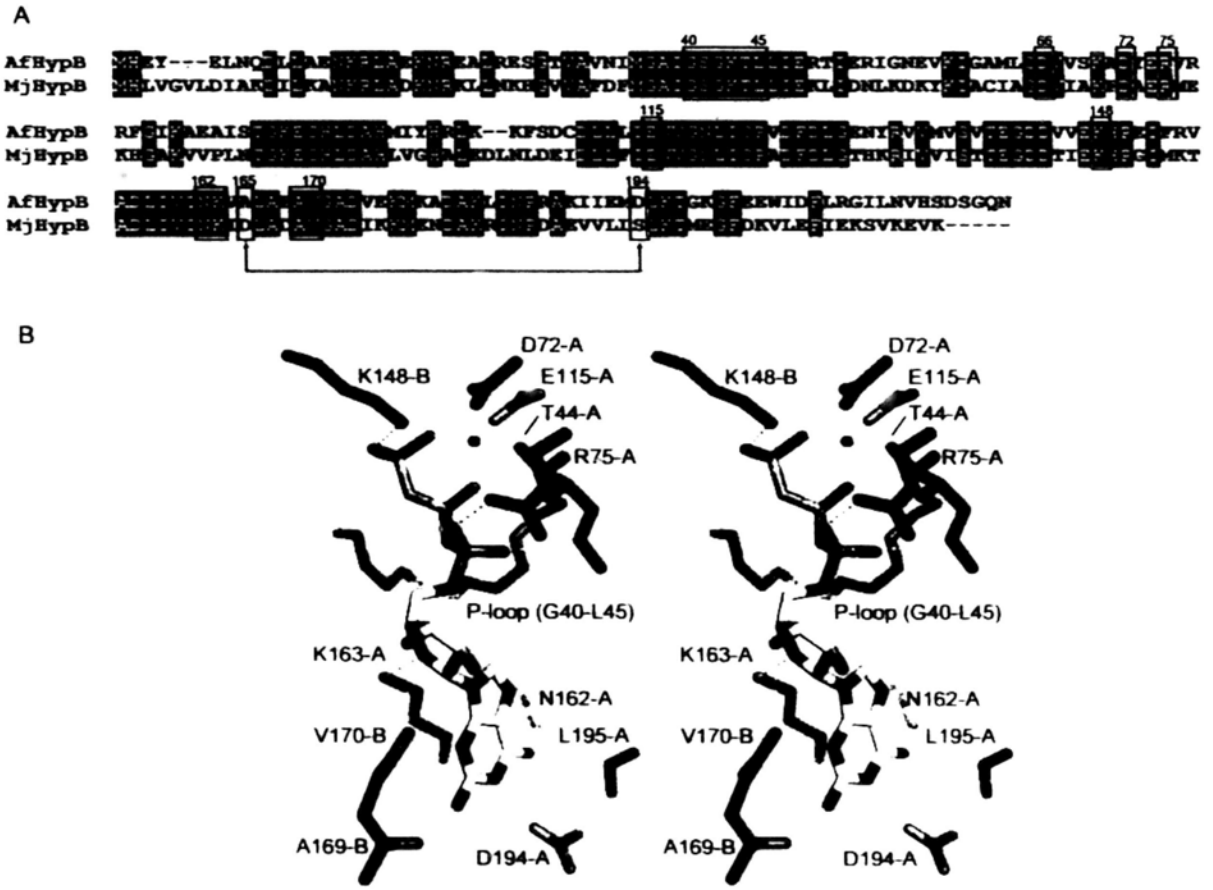

Figure 6.1 Modelling of the interactions between AfHypB and the bound GTP-γ-S/Mg^{2+}. (A) Sequence alignment of AfHypB and MjHypB. The key residues involved in GTP-binding and GTP-dependent dimerization are marked with red bars. Apart from the D194 played a role in recognition for the guanine base instead of aspartate in NKxD, the remaining residues are identical. (B) Residues of AfHypB involved in GTP-γ-S binding as shown in stereo diagram.

GTP-binding sites of AfHypB	Bound GTP-γ-S/ Mg^{2+}
D72Oδ1 (A)	Mg^{2+}
E115 Oε2 (A)	Mg^{2+}
T44 Oγ1 (A)	Mg^{2+}
K148 Nζ (B)	O2γ of GTP-γ-S
R75 Nη1 (A)	O2α of GTP-γ-S
L45 N (A)	O1α of GTP-γ-S
G40 N (A)	O3β of GTP-γ-S
S41 N (A)	O1β of GTP-γ-S
G42 N (A)	O3α of GTP-γ-S
K43 N (A)	O1β of GTP-γ-S
T44 N (A)	O2β of GTP-γ-S
L45 N (A)	O1α of GTP-γ-S
N162 Oδ1 (A)	N7 of GTP-γ-S
N162 Nδ2 (A)	O6 of GTP-γ-S
K163 Nζ (A)	O4 of GTP-γ-S
D194 Cγ (A)	N1 of GTP-γ-S
L195 N (A)	O6 of GTP-γ-S
A169 O (B)	N2 of GTP-γ-S
V170 O (B)	O3 of GTP-γ-S

Table 6.1 Summary of predicted interactions involved in recognition of GTP-γ-S to AfHypB. All residues contributing to dimerization from chain A and chain B are listed.

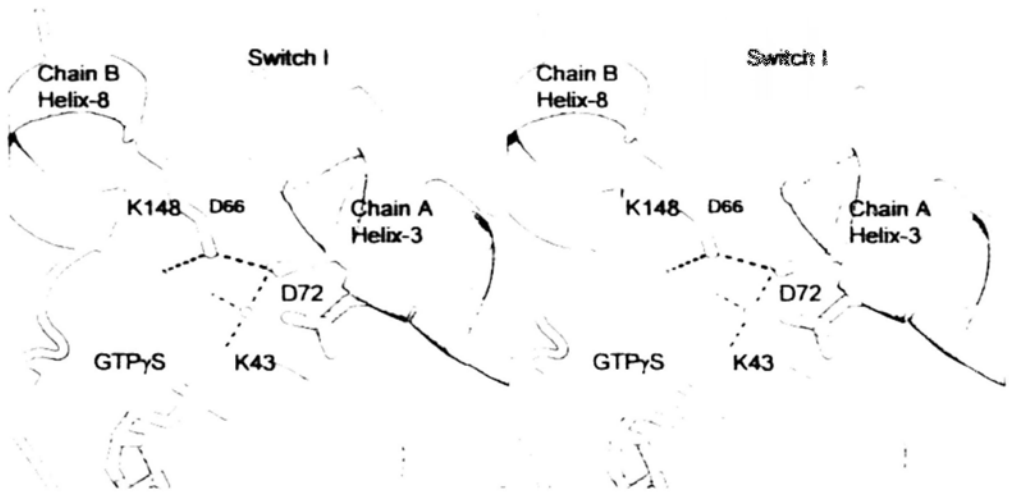

Figure 6.2 Conformational changes in the switch I loop and helix-3 faciliate GTP-dependent dimerization of HypB. The dimeric structure of AfHypB in complex with GTP-γ-S/Mg^{2+} was modeled by SWISS-MODEL using the stucture of GTP-γ-S-MjHypB as a template. The switch I loop and helix-3 of Chain A of GTP-γ-S-AfHypB is in green, while the apo-AfHypB is in white. Chain B of GTP-γ-S-AfHypB is in cyan. Upon GTP binding, the salt bridge between D66 and K43 is broken. As a result, the switch I loop moves away from the P-loop, allowing K148 of helix-8 to dock in a position to form a salt-bridge with the g-phosphate of GTP-γ-S. D72 of helix-3 swings towards the Mg binding site, and forms an inter-chain salt-bridge with K148. These extra interactions are likely to drive the dimerization of HypB.

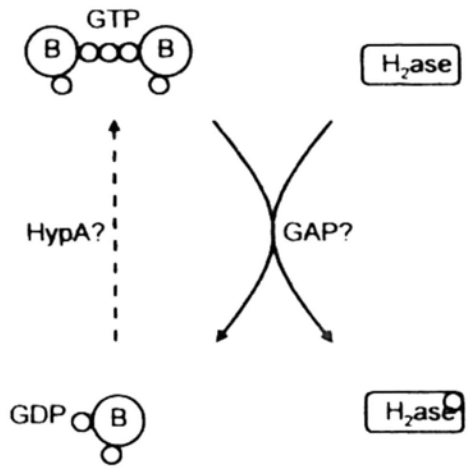

Figure 6.3 Model for Ni presenting via GTP hydrolysis by HypB. HypB acts as a GTP-dependent and dimerization-regulated switch upon GTP-binding and GTP-hydrolysis. GTP-dependent conformational changes are required for dimerization, which results in the formation of an extra Ni binding site. One Ni ion is released upon GTP-hydrolysis. HypA is likely to serve as a GEF for HypB.

References

(1994). "The CCP4 suite: programs for protein crystallography." Acta Crystallogr D Biol Crystallogr **50**(Pt 5): 760-3.

Altschul, S. F., W. Gish, et al. (1990). "Basic local alignment search tool." J Mol Biol **215**(3): 403-10.

Altschul, S. F., T. L. Madden, et al. (1997). "Gapped BLAST and PSI-BLAST: a new generation of protein database search programs." Nucleic Acids Res **25**(17): 3389-402.

Atanassova, A. and D. B. Zamble (2005). "Escherichia coli HypA is a zinc metalloprotein with a weak affinity for nickel." J Bacteriol **187**(14): 4689-97.

Binder, U., T. Maier, et al. (1996). "Nickel incorporation into hydrogenase 3 from Escherichia coli requires the precursor form of the large subunit." Arch Microbiol **165**(1): 69-72.

Blokesch, M., S. P. Albracht, et al. (2004). "The complex between hydrogenase-maturation proteins HypC and HypD is an intermediate in the supply of cyanide to the active site iron of [NiFe]-hydrogenases." J Mol Biol **344**(1): 155-67.

Blokesch, M., A. Paschos, et al. (2004). "Analysis of the transcarbamoylation-dehydration reaction catalyzed by the hydrogenase maturation proteins HypF and HypE." Eur J Biochem **271**(16): 3428-36.

Blokesch, M., A. Paschos, et al. (2002). "Metal insertion into NiFe-hydrogenases." Biochem Soc Trans **30**(4): 674-80.

Blokesch, M., M. Rohrmoser, et al. (2004). "HybF, a zinc-containing protein involved in NiFe hydrogenase maturation." J Bacteriol **186**(9): 2603-11.

Bock, A., P. W. King, et al. (2006). "Maturation of hydrogenases." Adv Microb Physiol **51**: 1-71.

Bourne, H. R., D. A. Sanders, et al. (1991). "The GTPase superfamily: conserved structure and molecular mechanism." Nature **349**(6305): 117-27.

Brunger, A. T., P. D. Adams, et al. (1998). "Crystallography & NMR system: A new software suite for macromolecular structure determination." Acta Crystallogr D Biol Crystallogr **54**(Pt 5): 905-21.

Casalot, L. and M. Rousset (2001). "Maturation of the [NiFe] hydrogenases." Trends Microbiol **9**(5): 228-37.

Cuff, J. A., M. E. Clamp, et al. (1998). "JPred: a consensus secondary structure prediction server." Bioinformatics **14**(10): 892-3.

Drapal, N. and A. Bock (1998). "Interaction of the hydrogenase accessory protein HypC with HycE, the large subunit of Escherichia coli hydrogenase 3 during enzyme maturation." Biochemistry **37**(9): 2941-8.

Ellman, G. L. (1959). "Tissue sulfhydryl groups." Arch Biochem Biophys **82**(1): 70-7.

Fisher, D. K. and T. J. Higgins (1994). "A sensitive, high-volume, colorimetric assay for protein phosphatases." Pharm Res **11**(5): 759-63.

Frey, M. (2002). "Hydrogenases: hydrogen-activating enzymes." Chembiochem **3**(2-3): 153-60.

Fu, C., J. W. Olson, et al. (1995). "HypB protein of Bradyrhizobium japonicum is a metal-binding GTPase capable of binding 18 divalent nickel ions per dimer." Proc Natl Acad Sci U S A **92**(6): 2333-7.

Gasper, R., A. Scrima, et al. (2006). "Structural insights into HypB, a GTP-binding protein that regulates metal binding." J Biol Chem **281**(37): 27492-502.

Geladopoulos, T. P., T. G. Sotiroudis, et al. (1991). "A malachite green colorimetric assay for protein phosphatase activity." Anal Biochem **192**(1): 112-6.

Happe, R. P., W. Roseboom, et al. (1997). "Biological activation of hydrogen." Nature **385**(6612): 126.

Hausinger, R. P. (1993). "Hydrogenase." In: The Biochemistry of Nickel: 50-105.

Hiratsuka, T. (1983). "New ribose-modified fluorescent analogs of adenine and guanine nucleotides available as substrates for various enzymes." Biochim Biophys Acta **742**(3): 496-508.

Hube, M., M. Blokesch, et al. (2002). "Network of hydrogenase maturation in Escherichia coli: role of accessory proteins HypA and HybF." J Bacteriol **184**(14): 3879-85.

Jacobi, A., R. Rossmann, et al. (1992). "The hyp operon gene products are required for the maturation of catalytically active hydrogenase isoenzymes in Escherichia coli." Arch Microbiol **158**(6): 444-51.

Kennedy, D. C., R. W. Herbst, et al. (2007). "A dynamic Zn site in Helicobacter pylori HypA: a potential mechanism for metal-specific protein activity." J Am Chem Soc **129**(1): 16-7.

Klenk, H. P., R. A. Clayton, et al. (1997). "The complete genome sequence of the hyperthermophilic, sulphate-reducing archaeon Archaeoglobus fulgidus." Nature **390**(6658): 364-70.

Kuchar, J. and R. P. Hausinger (2004). "Biosynthesis of metal sites." Chem Rev

104(2): 509-25.

Lanzetta, P. A., L. J. Alvarez, et al. (1979). "An improved assay for nanomole amounts of inorganic phosphate." Anal Biochem **100**(1): 95-7.

Leach, M. R., S. Sandal, et al. (2005). "Metal binding activity of the Escherichia coli hydrogenase maturation factor HypB." Biochemistry **44**(36): 12229-38.

Lee, M. H., H. S. Pankratz, et al. (1993). "Purification and characterization of Klebsiella aerogenes UreE protein: a nickel-binding protein that functions in urease metallocenter assembly." Protein Sci **2**(6): 1042-52.

Leipe, D. D., Y. I. Wolf, et al. (2002). "Classification and evolution of P-loop GTPases and related ATPases." J Mol Biol **317**(1): 41-72.

Liese, R. M. a. A. (2004). "Biotechnological applications of hydrogenases." Current Opinion in Biotechnology **15**: 343-348.

Lutz, S., A. Jacobi, et al. (1991). "Molecular characterization of an operon (hyp) necessary for the activity of the three hydrogenase isoenzymes in Escherichia coli." Mol Microbiol **5**(1): 123-35.

Magalon, A., M. Blokesch, et al. (2001). "Fidelity of metal insertion into hydrogenases." FEBS Lett **499**(1-2): 73-6.

Magalon, A. and A. Bock (2000). "Analysis of the HypC-hycE complex, a key intermediate in the assembly of the metal center of the Escherichia coli hydrogenase 3." J Biol Chem **275**(28): 21114-20.

Magalon, A. and A. Bock (2000). "Dissection of the maturation reactions of the [NiFe] hydrogenase 3 from Escherichia coli taking place after nickel incorporation." FEBS Lett **473**(2): 254-8.

Maier, T. and A. Bock (1996). "Nickel incorporation into hydrogenases." In: Mechanisms of Metallocenter Assembly. **11**: 173-192.

Maier, T., A. Jacobi, et al. (1993). "The product of the hypB gene, which is required for nickel incorporation into hydrogenases, is a novel guanine nucleotide-binding protein." J Bacteriol **175**(3): 630-5.

Maier, T., F. Lottspeich, et al. (1995). "GTP hydrolysis by HypB is essential for nickel insertion into hydrogenases of Escherichia coli." Eur J Biochem **230**(1): 133-8.

Mehta, N., S. Benoit, et al. (2003). "Roles of conserved nucleotide-binding domains in accessory proteins, HypB and UreG, in the maturation of nickel-enzymes required for efficient Helicobacter pylori colonization." Microb Pathog **35**(5): 229-34.

Mehta, N., J. W. Olson, et al. (2003). "Characterization of Helicobacter pylori nickel metabolism accessory proteins needed for maturation of both urease and hydrogenase." J Bacteriol **185**(3): 726-34.

Mulrooney, S. B. and R. P. Hausinger (2003). "Nickel uptake and utilization by microorganisms." FEMS Microbiol Rev **27**(2-3): 239-61.

Olson, J. W., C. Fu, et al. (1997). "The HypB protein from Bradyrhizobium japonicum can store nickel and is required for the nickel-dependent transcriptional regulation of hydrogenase." Mol Microbiol **24**(1): 119-28.

Olson, J. W. and R. J. Maier (2000). "Dual roles of Bradyrhizobium japonicum nickelin protein in nickel storage and GTP-dependent Ni mobilization." J Bacteriol **182**(6): 1702-5.

Olson, J. W. and R. J. Maier (2002). "Molecular hydrogen as an energy source for

Helicobacter pylori." Science **298**(5599): 1788-90.

Olson, J. W., N. S. Mehta, et al. (2001). "Requirement of nickel metabolism proteins HypA and HypB for full activity of both hydrogenase and urease in Helicobacter pylori." Mol Microbiol **39**(1): 176-82.

Paschos, A., A. Bauer, et al. (2002). "HypF, a carbamoyl phosphate-converting enzyme involved in [NiFe] hydrogenase maturation." J Biol Chem **277**(51): 49945-51.

Paschos, A., R. S. Glass, et al. (2001). "Carbamoylphosphate requirement for synthesis of the active center of [NiFe]-hydrogenases." FEBS Lett **488**(1-2): 9-12.

Reissmann, S., E. Hochleitner, et al. (2003). "Taming of a poison: biosynthesis of the NiFe-hydrogenase cyanide ligands." Science **299**(5609): 1067-70.

Rey, L., J. Imperial, et al. (1994). "Purification of Rhizobium leguminosarum HypB, a nickel-binding protein required for hydrogenase synthesis." J Bacteriol **176**(19): 6066-73.

Rossmann, R., M. Sauter, et al. (1994). "Maturation of the large subunit (HYCE) of Escherichia coli hydrogenase 3 requires nickel incorporation followed by C-terminal processing at Arg537." Eur J Biochem **220**(2): 377-84.

Van Veldhoven, P. P. and G. P. Mannaerts (1987). "Inorganic and organic phosphate measurements in the nanomolar range." Anal Biochem **161**(1): 45-8.

Vignais, P. M., B. Billoud, et al. (2001). "Classification and phylogeny of hydrogenases." FEMS Microbiol Rev **25**(4): 455-501.

Vignais, P. M. and A. Colbeau (2004). "Molecular biology of microbial

hydrogenases." Curr Issues Mol Biol **6**(2): 159-88.

Volbeda, A., M. H. Charon, et al. (1995). "Crystal structure of the nickel-iron hydrogenase from Desulfovibrio gigas." Nature **373**(6515): 580-7.

Volbeda A, F.-C. J. (2003). "The active site and catalytic mechanism of NiFe hydrogenases." Dalton Trans: 4030-4038.

Wakabayashi, H., K. M. Schmidt, et al. (2002). "Ca(2+) binding to both the heavy and light chains of factor VIII is required for cofactor activity." Biochemistry **41**(26): 8485-92.

Walker, J. E., M. Saraste, et al. (1982). "Distantly related sequences in the alpha- and beta-subunits of ATP synthase, myosin, kinases and other ATP-requiring enzymes and a common nucleotide binding fold." EMBO J **1**(8): 945-51.

Waugh, R. and D. H. Boxer (1986). "Pleiotropic hydrogenase mutants of Escherichia coli K12: growth in the presence of nickel can restore hydrogenase activity." Biochimie **68**(1): 157-66.

Wen, J., T. Arakawa, et al. (1996). "Size-exclusion chromatography with on-line light-scattering, absorbance, and refractive index detectors for studying proteins and their interactions." Anal Biochem **240**(2): 155-66.

Winter G, B. T., Lenz O, Jones AK, Forgber M, Friedrich B (2005). "A model system for [NiFe] hydrogenase maturation studuies: purification of an active site-containing hydrogenase large subunit without small subunit." FEBS Lett **579**: 4292-4296.